

A direct imaging method for inverse scattering problem of biharmonic wave with phased and phaseless data

Tielei Zhu* and Zhihao Ge

School of Mathematics and Statistics, Henan University, Kaifeng, Henan, 475004, China.

June 13, 2025

Abstract

This paper investigates the inverse biharmonic scattering problems of identifying the shape and location of the obstacle with phased and phaseless measurement data. A direct imaging method based on reverse time migration is proposed for reconstructing the extended obstacle with one of four types of boundary conditions on the obstacle. The newly developed imaging functions are constructed by utilizing merely one of various measurement data, including the scattered field, its normal derivative, the bending moment, the transverse force, its far-field and the phaseless total field. Our resolution analysis demonstrates that these imaging functions have a contrast when sampling points are near or far from the boundary of the obstacle. Numerical experiments are further presented to show the algorithm's efficiency to accurately reconstruct complex scatter geometries and its robustness to noise.

Keywords: Inverse biharmonic scattering problem, reverse time migration method, resolution analysis.

AMS subject classifications: 35Q74, 74J20

1 Introduction

The inverse obstacle scattering problems, which aims to determine the shape and location of the obstacle from the phased or phaseless measurement data have received significant attention in various fields including radar, medical imaging and geophysical exploration. Over the past decades, a large amount of numerical methods have been developed for the reconstruction of obstacles, such as Newton-type method in [17], Kirsch-Kress method in [10], linear sampling method in [3], factorization method in [21] and direct sampling method in [19, 27].

Most existing research has focused on inverse acoustic, elastic, and electromagnetic wave scattering problems. In contrast to these inverse scattering problems associated with second-order differential operators, limited work has been done on biharmonic inverse scattering problems involving the biharmonic wave equation (a fourth-order partial differential equation). However, the biharmonic inverse scattering problems have attracted growing research interest in recent years. Bourgeois and Recoquillay [2] established the uniqueness of Dirichlet-type (or Neumann-type) obstacles using multi-static data, namely the scattered field and its normal derivative. More recently, Dong and Li derived two uniqueness results based on phased far-field patterns and phaseless near-field data in [12]. Regarding numerical methods for biharmonic wave inverse problems, Bourgeois and Recoquillay introduced a linear sampling method for

*Corresponding author: zhutielei@126.com

obstacle reconstruction from multi-static near-field data. Chang and Guo [4] developed an optimization method for locating obstacles using measurement data of the scattered field and its Laplacian on a measured curve. Additionally, Guo *et al.* [14] proposed a linear sampling method employing far-field data. It is noteworthy that the aforementioned research addressed the frequency-domain problems. For the time domain problems, we refer to the recent work [13].

In this paper, we aim to develop new direct imaging method for the inverse biharmonic wave scattering problem with phased and phaseless data. Roughly speaking, the key to the direct imaging method lies in designing imaging functions that present distinct characteristics depending on whether the sampling point is near or far from the obstacle's boundary. This method has two primary advantages over iterative methods: (1) it does not require prior geometric assumptions about the scatterer, and (2) it avoids the need to solve the direct problems numerically. Very recently, Harris *et al.* proposed a direct imaging method for reconstructing the obstacle with the clamped boundary condition using far-field data in [15]. However, our imaging functions are based on reverse time migration method (RTM), which has been widely applied in seismic imaging and investigated in inverse scattering for acoustic, elastic and electromagnetic waves [5–7], and depend on only one of various measurement data, such as the scattered field, its normal derivative, the bending moment, the transverse force, its far-field and the phaseless total field. It should be emphasized that previous studies about the RTM can not be extended to the case of inverse biharmonic wave scattering directly. Furthermore, we propose novel imaging functions, which are involved only with the fundamental solution of the Helmholtz equation or an acoustic plane wave rather than the fundamental solution of the biharmonic wave equation or a biharmonic plane wave apart from the measurement data, and this formulation reduces computational complexity. We rely on new asymptotic behaviors to establish the resolution analysis of the imaging functions for the inverse scattering of the biharmonic wave, which is applicable to four types of boundary conditions.

The rest of the paper is organized as follows. In Section 2, we describe the direct and inverse scattering problems of biharmonic wave and introduce several important lemmas. Next, we propose and analyze the imaging functions with phased and phaseless data in Section 3 and Section 4, respectively. In Section 5, numerical experiments will be reported to show the validity of these methods.

2 Formulation of the biharmonic wave scattering problem

2.1 The direct scattering problem

Let $D \subset \mathbb{R}^2$ be a bounded domain with C^3 -smooth boundary Γ such that $D^c := \mathbb{R}^2 \setminus \overline{D}$ is connected. When the obstacle D is illuminated by the incident wave u^{in} , the scattered wave u^{sc} is excited, which satisfies the biharmonic wave equation

$$\Delta^2 u^{sc} - \kappa^4 u^{sc} = 0 \quad \text{in } D^c, \quad (2.1) \quad \text{eq:bi}$$

together with the boundary conditions

$$(\mathcal{B}_1 u^{sc}, \mathcal{B}_2 u^{sc}) = -(\mathcal{B}_1 u^{in}, \mathcal{B}_2 u^{in}) \quad \text{on } \Gamma, \quad (2.2) \quad \text{eq:boundary}$$

where $\kappa > 0$ is the wave number and \mathcal{B}_1 and \mathcal{B}_2 are boundary differential operators to be defined latter. Moreover, the scattered wave u^{sc} satisfies the Sommerfeld radiation condition

$$\lim_{r=|\mathbf{x}| \rightarrow \infty} \sqrt{r} \left(\frac{\partial u^{sc}}{\partial r} - i\kappa u^{sc} \right) = 0 \quad (2.3) \quad \text{eq:radiation}$$

uniformly for all $\hat{\mathbf{x}} = \mathbf{x}/|\mathbf{x}| \in \mathbb{S} := \{\mathbf{x} \in \mathbb{R}^2 : |\mathbf{x}| = 1\}$. As pointed out in [1], the Sommerfeld radiation condition for u^{sc} is sufficient. Due to (2.3), the scattered wave u^{sc} has the following asymptotic expansion:

$$u^{sc}(\mathbf{x}) = \frac{e^{\pi i/4}}{\sqrt{8\pi\kappa}} \frac{e^{i\kappa|\mathbf{x}|}}{|\mathbf{x}|^{1/2}} u^\infty(\hat{\mathbf{x}}) + O\left(\frac{1}{|\mathbf{x}|^{3/2}}\right) \quad |\mathbf{x}| \rightarrow \infty, \quad (2.4) \quad \text{eq:asy}$$

where u^∞ is defined as the far-field pattern of the scattered wave u^{sc} .

To clarify the definitions of the boundary differential operators \mathcal{B}_1 and \mathcal{B}_2 , let $\mathbf{n} = (n_1, n_2)^T$ be the exterior unit normal vector of the boundary Γ . Define the boundary operators M_0v and N_0v as follows:

$$M_0v = n_1^2 \frac{\partial^2 v}{\partial x_1^2} + 2n_1 n_2 \frac{\partial^2 v}{\partial x_1 \partial x_2} + n_2^2 \frac{\partial^2 v}{\partial x_2^2}$$

and

$$N_0v = -\left\{ \left(\frac{\partial^2 v}{\partial x_1^2} - \frac{\partial^2 v}{\partial x_2^2} \right) n_1 n_2 - \frac{\partial^2 v}{\partial x_1 \partial x_2} (n_1^2 - n_2^2) \right\}.$$

Then the boundary operators Mv and Nv are defined as follows:

$$Mv = \nu \Delta v + (1 - \nu) M_0v$$

and

$$Nv = -\partial_{\mathbf{n}} \Delta v - (1 - \nu) \partial_s N_0v,$$

where $\nu \in [0, \frac{1}{2})$ is the Poisson ratio. Here the normal and tangential derivatives $\partial_{\mathbf{n}}$ and ∂_s are given by

$$\partial_{\mathbf{n}} = n_1 \partial_{x_1} + n_2 \partial_{x_2} \quad \text{and} \quad \partial_s = -n_2 \partial_{x_1} + n_1 \partial_{x_2}.$$

From a physical perspective, Mv is the bending moment, whereas Nv is the transverse force (consisting of the shear force and twisting moment) [9].

In this paper, we consider the following boundary conditions:

- I. Clamped boundary condition: $\mathcal{B}_1 = I$ and $\mathcal{B}_2 = \partial_{\mathbf{n}}$
- II. Simply supported boundary condition: $\mathcal{B}_1 = I$ and $\mathcal{B}_2 = M$
- III. Roller supported boundary condition: $\mathcal{B}_1 = \partial_{\mathbf{n}}$ and $\mathcal{B}_2 = N$
- IV. Free boundary condition: $\mathcal{B}_1 = M$ and $\mathcal{B}_2 = N$.

It is important to emphasize that the aforementioned boundary conditions, rooted in plate theory, impose different requirements on the domain D . Specifically, the domain D should be at least of class C^2 in the boundary conditions I-III, whereas the domain should be at least of class C^3 in the boundary condition IV, which is necessary in the proof of Theorem 3.4 in [1].

The direct problem has been studied in [1]. First, we state the well-posedness of a more general boundary value problem

$$\Delta^2 w - \kappa^4 w = 0 \quad \text{in } D^c, \tag{2.5a}$$

$$(\mathcal{B}_1 w, \mathcal{B}_2 w) = (f, g) \quad \text{on } \Gamma, \tag{2.5b}$$

$$\lim_{r \rightarrow \infty} \sqrt{r} \left(\frac{\partial w}{\partial r} - i\kappa w \right) = 0, \tag{2.5c}$$

which could become ^{eq:bi}(2.1)-^{eq:radiation}(2.3) if $(f, g) = -(\mathcal{B}_1 u^{in}, \mathcal{B}_2 u^{in})$.

lem:well

Lemma 2.1 (see [1]). *The boundary value problem ^{eq:bvp}(2.5) admits a unique solution w in $H_{\text{loc}}^2(D^c)$*

- for any $(f, g) \in H^{3/2}(\Gamma) \times H^{1/2}(\Gamma)$ and $\kappa > 0$ if $\mathcal{B}_1 = I$ and $\mathcal{B}_2 = \partial_{\mathbf{n}}$. Moreover, the the solution satisfies the following estimation:

$$\begin{aligned} \|w\|_{H_{\text{loc}}^2(D^c)} &\leq C(\|f\|_{H^{3/2}(\Gamma)} + \|g\|_{H^{1/2}(\Gamma)}), \\ \|Mw\|_{H^{-1/2}(\Gamma)} + \|Nw\|_{H^{-3/2}(\Gamma)} &\leq C(\|f\|_{H^{3/2}(\Gamma)} + \|g\|_{H^{1/2}(\Gamma)}), \end{aligned}$$

where $C > 0$ is some constant depending on wave number κ and the domain D .

- for any $(f, g) \in H^{3/2}(\Gamma) \times H^{-1/2}(\Gamma)$ and $\kappa > 0$ if $\mathcal{B}_1 = I$ and $\mathcal{B}_2 = M$. Moreover, the the solution satisfies the following estimation:

$$\begin{aligned} \|w\|_{H_{\text{loc}}^2(D^c)} &\leq C(\|f\|_{H^{3/2}(\Gamma)} + \|g\|_{H^{-1/2}(\Gamma)}), \\ \|\partial_{\mathbf{n}}w\|_{H^{1/2}(\Gamma)} + \|Nw\|_{H^{-3/2}(\Gamma)} &\leq C(\|f\|_{H^{3/2}(\Gamma)} + \|g\|_{H^{-1/2}(\Gamma)}), \end{aligned}$$

where $C > 0$ is some constant depending on wave number κ and the domain D .

- for any $(f, g) \in H^{1/2}(\Gamma) \times H^{-3/2}(\Gamma)$ and $\kappa > 0$ if $\mathcal{B}_1 = \partial_{\mathbf{n}}$ and $\mathcal{B}_2 = N$. Moreover, the the solution satisfies the following estimation:

$$\begin{aligned} \|w\|_{H_{\text{loc}}^2(D^c)} &\leq C(\|f\|_{H^{1/2}(\Gamma)} + \|g\|_{H^{-3/2}(\Gamma)}), \\ \|w\|_{H^{3/2}(\Gamma)} + \|Mw\|_{H^{-1/2}(\Gamma)} &\leq C(\|f\|_{H^{1/2}(\Gamma)} + \|g\|_{H^{-3/2}(\Gamma)}), \end{aligned}$$

where $C > 0$ is some constant depending on wave number κ and the domain D .

- for any $(f, g) \in H^{-1/2}(\Gamma) \times H^{-3/2}(\Gamma)$ and $\kappa > 0$ except an at most countable sequence of positive wave number $(\kappa_j)_{j \in \mathbb{N}} \subset \mathbb{R}_{>0}$ without finite accumulation point, if $\mathcal{B}_1 = M$ and $\mathcal{B}_2 = N$. Moreover, the the solution satisfies the following estimation:

$$\begin{aligned} \|w\|_{H_{\text{loc}}^2(D^c)} &\leq C(\|f\|_{H^{-1/2}(\Gamma)} + \|g\|_{H^{-3/2}(\Gamma)}), \\ \|w\|_{H^{3/2}(\Gamma)} + \|\partial_{\mathbf{n}}w\|_{H^{1/2}(\Gamma)} &\leq C(\|f\|_{H^{-1/2}(\Gamma)} + \|g\|_{H^{-3/2}(\Gamma)}), \end{aligned}$$

where $C > 0$ is some constant depending on wave number κ and the domain D .

In this paper, to ensure the uniqueness of the scattering problem [\(2.5\)](#)^{eq:bvp}, we always assume that κ is not in the discrete set of wave number for boundary condition IV.

The fundamental solution to the biharmonic wave equation is given by

$$G(\mathbf{x}, \mathbf{y}) = \frac{1}{2\kappa^2} (\Phi_{i\kappa}(\mathbf{x}, \mathbf{y}) - \Phi_{\kappa}(\mathbf{x}, \mathbf{y})), \quad (2.6) \quad \text{eq:funda-bi}$$

i.e., it satisfies

$$\Delta^2 G(\mathbf{x}, \mathbf{y}) - \kappa^4 G(\mathbf{x}, \mathbf{y}) = -\delta(\mathbf{x} - \mathbf{y}).$$

Here $\Phi_{\kappa}(\mathbf{x}, \mathbf{y}) = \frac{i}{4} H_0^{(1)}(\kappa|\mathbf{x} - \mathbf{y}|)$ is the fundamental solution of two-dimensional Helmholtz equation and $H_0^{(1)}$ is the Hankel function of the first kind with the order zero.

Let us introduce the Green formula (see [18]). Assume that a bounded domain Ω is C^2 -smooth with \mathbf{n} the outward unit normal. For $v \in H^2(\Omega, \Delta^2) := \{v \in H^2(\Omega) : \Delta^2 v \in L^2(\Omega)\}$ and $w \in H^2(\Omega)$, we can have

$$\int_{\Omega} (\Delta^2 v) w \, d\mathbf{x} = a_{\Omega}(v, w) - \int_{\partial\Omega} [(Mv)\partial_{\mathbf{n}}w + (Nv)w] \, ds, \quad (2.7) \quad \text{eq:green-1}$$

where

$$a_{\Omega}(v, w) = \nu \int_{\Omega} \Delta v \Delta w \, d\mathbf{x} + (1 - \nu) \int_{\Omega} \left(\frac{\partial^2 v}{\partial x_1^2} \frac{\partial^2 w}{\partial x_1^2} + 2 \frac{\partial^2 v}{\partial x_1 \partial x_2} \frac{\partial^2 w}{\partial x_1 \partial x_2} + \frac{\partial^2 v}{\partial x_2^2} \frac{\partial^2 w}{\partial x_2^2} \right) \, d\mathbf{x}.$$

Similarly, for $v, w \in H^2(\Omega, \Delta^2)$ we could obtain

$$\int_{\Omega} [w(\Delta^2 v) - v(\Delta^2 w)] \, d\mathbf{x} = \int_{\partial\Omega} \left\{ [(Mw)\partial_{\mathbf{n}}v + (Nw)v] - [(Mv)\partial_{\mathbf{n}}w + (Nv)w] \right\} \, ds. \quad (2.8) \quad \text{eq:green-2}$$

Based on the fundamental solution $G(\mathbf{x}, \mathbf{y})$ and Green formula, we can get the representations of the scattered field and its far-field pattern in the following lemma, which is similar to Proposition 1 in [2] and Theorem 3.2 in [12]. For the sake of completeness, we provide a proof.

lem:rep

Lemma 2.2. Assume that $w \in H_{\text{loc}}^2(D^c)$ is the radiation solution, i.e., it satisfies (2.1) and (2.3), and w^∞ is far-field pattern of w . Then

$$w(\mathbf{x}) = \int_{\Gamma} \left\{ [G(\mathbf{x}, \mathbf{y})Nw(\mathbf{y}) + [\partial_{\mathbf{n}(\mathbf{y})}G(\mathbf{x}, \mathbf{y})]Mw(\mathbf{y})] - [[N_{\mathbf{y}}G(\mathbf{x}, \mathbf{y})]w(\mathbf{y}) + [M_{\mathbf{y}}G(\mathbf{x}, \mathbf{y})]\partial_{\mathbf{n}}w(\mathbf{y})] \right\} ds(\mathbf{y}) \quad \mathbf{x} \in D^c, \quad (2.9) \quad \text{eq:Green-rep}$$

$$w^\infty(\hat{\mathbf{x}}) = -\frac{1}{2\kappa^2} \int_{\Gamma} \left\{ [e^{-i\kappa\hat{\mathbf{x}}\cdot\mathbf{y}}Nw(\mathbf{y}) + (\partial_{\mathbf{n}(\mathbf{y})}e^{-i\kappa\hat{\mathbf{x}}\cdot\mathbf{y}})Mw(\mathbf{y})] - [(N_{\mathbf{y}}e^{-i\kappa\hat{\mathbf{x}}\cdot\mathbf{y}})w(\mathbf{y}) + (M_{\mathbf{y}}e^{-i\kappa\hat{\mathbf{x}}\cdot\mathbf{y}})\partial_{\mathbf{n}}w(\mathbf{y})] \right\} ds(\mathbf{y}) \quad \hat{\mathbf{x}} \in \mathbb{S}. \quad (2.10) \quad \text{eq:far-rep}$$

Proof. Let $\mathbf{x} \in D^c$ and choose a sufficiently large $r > 0$ and a sufficiently small $\rho > 0$ such that $\overline{D} \subset B(\mathbf{0}, r)$ and $\overline{B(\mathbf{x}, \rho)} \subset B(\mathbf{0}, r) \setminus \overline{D}$, where the unit normal \mathbf{n} of $\partial B(\mathbf{0}, r)$ is directed toward the outside of the ball $B(\mathbf{0}, r)$ and the unit normal \mathbf{n} of $\partial B(\mathbf{x}, \rho)$ is directed toward the inside of the ball $B(\mathbf{x}, \rho)$. We apply the Green formula (2.8) to w and $G(\mathbf{x}, \cdot)$ in $D_{\rho, r} := B(\mathbf{0}, r) \setminus (\overline{D} \cup \overline{B(\mathbf{x}, \rho)})$ to obtain

$$0 = \int_{D_{\rho, r}} [G(\mathbf{x}, \mathbf{y})\Delta^2 w(\mathbf{y}) - w(\mathbf{y})\Delta_{\mathbf{y}}^2 G(\mathbf{x}, \mathbf{y})] d\mathbf{y} = \int_{\Gamma \cup \partial B(\mathbf{x}, \rho) \cup \partial B(\mathbf{0}, r)} \mathcal{U}(\mathbf{x}, \mathbf{y}) ds(\mathbf{y}) \\ = \left(-\int_{\Gamma} + \int_{\partial B(\mathbf{x}, \rho)} + \int_{\partial B(\mathbf{0}, r)} \right) \mathcal{U}(\mathbf{x}, \mathbf{y}) ds(\mathbf{y}), \quad (2.11) \quad \text{eq:greendr}$$

where

$$\mathcal{U}(\mathbf{x}, \mathbf{y}) = [(M_{\mathbf{y}}G(\mathbf{x}, \mathbf{y}))\partial_{\mathbf{n}(\mathbf{y})}w(\mathbf{y}) + (N_{\mathbf{y}}G(\mathbf{x}, \mathbf{y}))w(\mathbf{y})] - [\partial_{\mathbf{n}(\mathbf{y})}G(\mathbf{x}, \mathbf{y})(M_{\mathbf{y}}w(\mathbf{y})) + G(\mathbf{x}, \mathbf{y})(N_{\mathbf{y}}w(\mathbf{y}))].$$

It follows from Propositions 2.1 and 2.2 in [1] that the radiation solution w has the decomposition $w = w^{pr} + w^{ev}$ and their asymptotic behaviors are

$$|w^{pr}(\mathbf{x})| = O(|\mathbf{x}|^{-1/2}), \quad |\partial_r w^{pr} - i\kappa w^{pr}| = O(|\mathbf{x}|^{-3/2}) \quad \text{and} \quad |w^{ev}(\mathbf{x})| = O(e^{-\kappa|\mathbf{x}|}) \quad \text{as} \quad |\mathbf{x}| \rightarrow \infty,$$

uniformly with respect to $\theta \in [0, 2\pi)$. Note that the boundary operators M and N in the polar coordinates can be rewritten as follows:

$$Mw = \Delta w - (1 - \nu) \left(\frac{1}{r} \frac{\partial w}{\partial r} + \frac{1}{r^2} \frac{\partial^2 w}{\partial \theta^2} \right), \quad (2.12) \quad \text{eq:Mpolar}$$

$$Nw = -\frac{\partial}{\partial r} \Delta w - (1 - \nu) \frac{1}{r^2} \frac{\partial}{\partial \theta} \left(\frac{\partial^2 w}{\partial r \partial \theta} - \frac{1}{r} \frac{\partial w}{\partial \theta} \right). \quad (2.13) \quad \text{eq:Npolar}$$

Then we have

$$Mw(\mathbf{x}) = -\kappa^2 w^{pr}(\mathbf{x}) + O(r^{-3/2}) \quad \text{and} \quad Nw(\mathbf{x}) = \kappa^2 \partial_r w^{pr}(\mathbf{x}) + O(r^{-5/2}) \quad \text{as} \quad r = |\mathbf{x}| \rightarrow \infty, \quad (2.14) \quad \text{eq:MNw}$$

where we use the fact that $\Delta w^{pr} + \kappa^2 w^{pr} = 0$ in D^c . Similarly, the asymptotic behaviors of the Hankel function [25, Chapter 7, section 4.1] as $z \rightarrow \infty$, i.e.,

$$H_n^{(1)}(z) = \sqrt{\frac{2}{\pi z}} e^{i(z - n\pi/2 - \pi/4)} (1 + O(|z|^{-1})) \quad \text{for} \quad \arg z \in [-\frac{\pi}{2}, \frac{\pi}{2}] \quad \text{and} \quad n = 0, 1, \dots, \quad (2.15) \quad \text{eq:Hankel}$$

and the recurrence relation

$$(H_m^{(1)})'(z) = H_{m-1}^{(1)}(z) - \frac{m}{z} H_m^{(1)}(z)$$

imply that

$$M_{\mathbf{y}}G(\mathbf{x}, \mathbf{y}) = -\kappa^2 G^{pr}(\mathbf{x}, \mathbf{y}) + O(|\mathbf{y}|^{-3/2}) \quad \text{as} \quad |\mathbf{y}| \rightarrow \infty, \quad (2.16) \quad \text{eq:MG}$$

and

$$N_{\mathbf{y}}G(\mathbf{x}, \mathbf{y}) = \kappa^2 \partial_{|\mathbf{y}|} G^{pr}(\mathbf{x}, \mathbf{y}) + O(|\mathbf{y}|^{-5/2}) \quad \text{as } |\mathbf{y}| \rightarrow \infty, \quad (2.17) \quad \text{eq:NG}$$

where $G^{pr}(\mathbf{x}, \mathbf{y}) = -1/(2\kappa^2)\Phi_\kappa(\mathbf{x}, \mathbf{y})$. Letting $r \rightarrow \infty$ and combining (2.14)-(2.17), we have

$$\begin{aligned} & \lim_{r \rightarrow \infty} \int_{\partial B(\mathbf{0}, r)} \mathcal{U}(\mathbf{x}, \mathbf{y}) \, ds(\mathbf{y}) \\ &= 2\kappa^2 \lim_{r \rightarrow \infty} \int_{\partial B(\mathbf{0}, r)} \left\{ -G^{pr}(\mathbf{x}, \mathbf{y}) [\partial_{\mathbf{n}(\mathbf{y})} w^{pr}(\mathbf{y}) - i\kappa w^{pr}(\mathbf{y})] \right. \\ & \quad \left. + w^{pr}(\mathbf{y}) [\partial_{\mathbf{n}(\mathbf{y})} G^{pr}(\mathbf{x}, \mathbf{y}) - i\kappa G^{pr}(\mathbf{x}, \mathbf{y})] \right\} ds(\mathbf{y}) = 0, \end{aligned} \quad (2.18) \quad \text{eq:greendr-1}$$

since that $\Phi_\kappa(\mathbf{x}, \mathbf{y})$ satisfies the Sommerfeld radiation condition (2.3). Observe that for $\mathbf{y} \in \partial B(\mathbf{x}, \rho)$ the following formulas hold:

$$\begin{aligned} \partial_{\mathbf{n}(\mathbf{y})} G(\mathbf{x}, \mathbf{y}) &= -\frac{i}{8\kappa} [iH_1^{(1)}(i\kappa\rho) - H_1^{(1)}(\kappa\rho)], \\ M_{\mathbf{y}}G(\mathbf{x}, \mathbf{y}) &= \frac{i}{8} [H_0^{(1)}(i\kappa\rho) + H_0^{(1)}(\kappa\rho)] + (1-\nu)\frac{1}{\rho}\partial_{\mathbf{n}(\mathbf{y})}G(\mathbf{x}, \mathbf{y}), \\ N_{\mathbf{y}}G(\mathbf{x}, \mathbf{y}) &= \frac{i}{8} \left[\frac{\partial}{\partial\rho} H_0^{(1)}(i\kappa\rho) + \frac{\partial}{\partial\rho} H_0^{(1)}(\kappa\rho) \right]. \end{aligned}$$

Using the asymptotic behaviors of Hankel functions as $\rho \rightarrow 0$, we obtain

$$\lim_{\rho \rightarrow 0} \int_{\partial B(\mathbf{x}, \rho)} \mathcal{U}(\mathbf{x}, \mathbf{y}) \, ds(\mathbf{y}) = \lim_{\rho \rightarrow 0} \int_{\partial B(\mathbf{x}, \rho)} (N_{\mathbf{y}}G(\mathbf{x}, \mathbf{y}))w(\mathbf{y}) \, ds(\mathbf{y}) = -w(\mathbf{x}). \quad (2.19) \quad \text{eq:greendr-2}$$

The Green representation (2.9) follows by substituting (2.18) and (2.19) into (2.11). By the representation (2.9) we derive (2.10) due to the definition of the far-field pattern and the asymptotic behaviors of the Hankel functions. \square

Moreover, we have the following property of the radiation solution, which is corresponding to the sign property of the imaginary part of the Dirichlet-to-Neumann mapping in the acoustic and elastic wave scattering problems (c.f. [5, Lemma 3.3] and [7, Lemma 3.5]) and has been proved essentially in Proposition 3.2 of [1]. For the convenience of the readers, we provide the details here.

lem:sign

Lemma 2.3. Let w satisfy (2.1) and (2.3) and w^∞ be the far-field pattern of w . Then

$$\text{Im} \int_{\Gamma} [\bar{w} Nw + \partial_{\mathbf{n}} \bar{w} Mw] \, ds = \text{Im} \int_{\Gamma} [\bar{w} Nw - M\bar{w} \partial_{\mathbf{n}} w] \, ds = \frac{\kappa^2}{4\pi} \int_{\mathbb{S}} |w^\infty|^2 \, ds.$$

Proof. It suffices to prove

$$\text{Im} \int_{\Gamma} [\bar{w} Nw + \partial_{\mathbf{n}} \bar{w} Mw] \, ds = \frac{\kappa^2}{4\pi} \int_{\mathbb{S}} |w^\infty|^2 \, ds,$$

due to the fact that $\text{Im}(z_1 + z_2) = \text{Im}(z_1 - \bar{z}_2)$ for any $z_1, z_2 \in \mathbb{C}$. Let $B(\mathbf{0}, r)$ denote an open disk centered at the origin with radius r such that the disk $B(\mathbf{0}, r)$ contains \bar{D} . By the Green formula (2.7) in $B_r \setminus \bar{D}$, we have

$$\left(\int_{\partial B(\mathbf{0}, r)} - \int_{\Gamma} \right) [\bar{w} Nw + \partial_{\mathbf{n}} \bar{w} Mw] \, ds = a_{D_r}(w, \bar{w}) - \kappa^4 \int_{D_r} |w|^2 \, d\mathbf{x}$$

where $D_r := B(\mathbf{0}, r) \setminus \bar{D}$, which implies

$$\text{Im} \int_{\Gamma} [\bar{w} Nw + \partial_{\mathbf{n}} \bar{w} Mw] \, ds = \text{Im} \int_{\partial B(\mathbf{0}, r)} [\bar{w} Nw + \partial_{\mathbf{n}} \bar{w} Mw] \, ds \quad (2.20) \quad \text{eq:lem-1}$$

From the asymptotic behavior of w , i.e., (2.4) with u^∞ (or u^{sc}) replaced by w^∞ (or w), together with the identities (2.12) and (2.13), we can obtain the asymptotic behaviors of Mw and Nw as follows:

$$\begin{aligned} Mw(\mathbf{x}) &= -\kappa^2 \frac{e^{i\pi/4}}{\sqrt{8\pi\kappa}} \frac{e^{i\kappa|\mathbf{x}|}}{|\mathbf{x}|^{1/2}} w^\infty(\hat{\mathbf{x}}) + O(|\mathbf{x}|^{-3/2}) \quad |\mathbf{x}| \rightarrow \infty, \\ Nw(\mathbf{x}) &= i\kappa^3 \frac{e^{i\pi/4}}{\sqrt{8\pi\kappa}} \frac{e^{i\kappa|\mathbf{x}|}}{|\mathbf{x}|^{1/2}} w^\infty(\hat{\mathbf{x}}) + O(|\mathbf{x}|^{-3/2}) \quad |\mathbf{x}| \rightarrow \infty. \end{aligned}$$

Straightforward calculations shows that

$$\overline{w}(\mathbf{x}) Nw(\mathbf{x}) + Mw(\mathbf{x}) \partial_r \overline{w}(\mathbf{x}) = \frac{i\kappa^2}{4\pi} |w^\infty(\hat{\mathbf{x}})|^2 + O(|\mathbf{x}|^{-2}) \quad |\mathbf{x}| \rightarrow \infty.$$

Taking the imaginary part of (2.20) and the limits $r = |\mathbf{x}| \rightarrow \infty$ yield the conclusion. \square

2.2 The inverse scattering problems for extended obstacles

Let B_r (or B_s) be the open disk with center at the origin and radius $R_r > 0$ (or $R_s > 0$) such that $\overline{D} \subset B_r$ (or $D \subset B_s$), and we denote by Γ_r (or Γ_s) the boundary of B_r (or B_s) with \mathbf{n}_r being the outward unit normal of Γ_r . Let Ω be the sampling domain containing the closure \overline{D} of the obstacle D . We assume that Ω is entirely contained within either B_r (or B_s), i.e., $\overline{\Omega} \subset B_r$ (or B_s).

Consider the plane wave $u^{in}(\mathbf{x}, \mathbf{d}) = e^{i\kappa\mathbf{x}\cdot\mathbf{d}}$ as the incident wave, where $\mathbf{d} \in \mathbb{S}$ is the incident direction, and we denote by $u^{sc}(\mathbf{x}, \mathbf{d})$ and $u^\infty(\hat{\mathbf{x}}, \mathbf{d})$ the scattered field and far-field pattern respectively. Besides, we also consider the point source located on Γ_s as the incident wave. Let $u^{in}(\mathbf{x}, \mathbf{x}_s) = \Phi_\kappa(\mathbf{x}, \mathbf{x}_s)$ ($\mathbf{x}_s \in \Gamma_s$) and then $u^{sc}(\mathbf{x}, \mathbf{x}_s)$ and $u^\infty(\hat{\mathbf{x}}, \mathbf{x}_s)$ are the scattered field and far-field pattern respectively. Define $u(\mathbf{x}, \mathbf{x}_s) := u^{sc}(\mathbf{x}, \mathbf{x}_s) + u^{in}(\mathbf{x}, \mathbf{x}_s)$ as the total field.

In the remainder of this paper, we are interested in the following eleven inverse biharmonic scattering problems.

- **IP-1:** Determine the shape and location of the obstacle D from $u^{sc}(\mathbf{x}_r, \mathbf{x}_s)$ for all observation points $\mathbf{x}_r \in \Gamma_r$ and all source points $\mathbf{x}_s \in \Gamma_s$.
- **IP-2:** Determine the shape and location of the obstacle D from $\partial_{\mathbf{n}(\mathbf{x}_r)} u^{sc}(\mathbf{x}_r, \mathbf{x}_s)$ for all observation points $\mathbf{x}_r \in \Gamma_r$ and all source points $\mathbf{x}_s \in \Gamma_s$.
- **IP-3:** Determine the shape and location of the obstacle D from $M_{\mathbf{x}_r} u^{sc}(\mathbf{x}_r, \mathbf{x}_s)$ for all observation points $\mathbf{x}_r \in \Gamma_r$ and all source points $\mathbf{x}_s \in \Gamma_s$.
- **IP-4:** Determine the shape and location of the obstacle D from $N_{\mathbf{x}_r} u^{sc}(\mathbf{x}_r, \mathbf{x}_s)$ for all observation points $\mathbf{x}_r \in \Gamma_r$ and all source points $\mathbf{x}_s \in \Gamma_s$.
- **IP-5:** Determine the shape and location of the obstacle D from $u^{sc}(\mathbf{x}_r, \mathbf{d})$ for all observation points $\mathbf{x}_r \in \Gamma_r$ and all incident directions $\mathbf{d} \in \mathbb{S}$.
- **IP-6:** Determine the shape and location of the obstacle D from $\partial_{\mathbf{n}(\mathbf{x}_r)} u^{sc}(\mathbf{x}_r, \mathbf{d})$ for all observation points $\mathbf{x}_r \in \Gamma_r$ and all incident directions $\mathbf{d} \in \mathbb{S}$.
- **IP-7:** Determine the shape and location of the obstacle D from $M_{\mathbf{x}_r} u^{sc}(\mathbf{x}_r, \mathbf{d})$ for all observation points $\mathbf{x}_r \in \Gamma_r$ and all incident directions $\mathbf{d} \in \mathbb{S}$.
- **IP-8:** Determine the shape and location of the obstacle D from $N_{\mathbf{x}_r} u^{sc}(\mathbf{x}_r, \mathbf{d})$ for all observation points $\mathbf{x}_r \in \Gamma_r$ and all incident directions $\mathbf{d} \in \mathbb{S}$.
- **IP-9:** Determine the shape and location of the obstacle D from $u^\infty(\hat{\mathbf{x}}, \mathbf{x}_s)$ for all observation directions $\hat{\mathbf{x}} \in \mathbb{S}$ and all source points $\mathbf{x}_s \in \Gamma_s$.

- **IP-10:** Determine the shape and location of the obstacle D from $u^\infty(\hat{\mathbf{x}}, \mathbf{d})$ for all observation directions $\hat{\mathbf{x}} \in \mathbb{S}$ and all incident directions $\mathbf{d} \in \mathbb{S}$.
- **IP-11:** Determine the shape and location of the obstacle D from $|u(\mathbf{x}_r, \mathbf{x}_s)|$ for all observation points $\mathbf{x}_r \in \Gamma_r$ and all source points $\mathbf{x}_s \in \Gamma_s$.

The inverse scattering problems can be divided into two classes: phased and phaseless inverse scattering problems. For phased inverse scattering problems, numerous studies have focused on reconstructing obstacles from the scattered field generated by point sources or far-field patterns generated by plane waves. Furthermore, we notice that some works about the direct imaging method are concerned with the case of the Cauchy data (i.e., the scattered field and its normal derivative) generated by point sources in [16] and those generated by plane waves in [24]. Similarly, for phaseless inverse scattering problems, numerical reconstruction could be based on various measurement data such as the phaseless far-field data generated by point sources [28], the phaseless near-field data generated by plane waves [29], the phaseless near-field data generated by point sources [8] and the phaseless far-field data generated by the superposition of the plane waves and a point source [20].

3 The direct imaging method with phased data

sec:phased

This section is devoted to the direct imaging method for **IP-1** through **IP-10**. To address the aforementioned ten inverse problems **IP-1** through **IP-10**, the following imaging functions are defined:

$$I_1(z) = -2\kappa^4 \operatorname{Im} \int_{\Gamma_r} \int_{\Gamma_s} \Phi_\kappa(\mathbf{z}, \mathbf{x}_r) \Phi_\kappa(\mathbf{z}, \mathbf{x}_s) \overline{u^{sc}(\mathbf{x}_r, \mathbf{x}_s)} \, ds(\mathbf{x}_s) ds(\mathbf{x}_r), \quad (3.1) \quad \text{fun-1}$$

$$I_2(z) = -2\kappa^3 \operatorname{Re} \int_{\Gamma_r} \int_{\Gamma_s} \Phi_\kappa(\mathbf{z}, \mathbf{x}_r) \Phi_\kappa(\mathbf{z}, \mathbf{x}_s) \overline{\partial_{\mathbf{n}(\mathbf{x}_r)} u^{sc}(\mathbf{x}_r, \mathbf{x}_s)} \, ds(\mathbf{x}_s) ds(\mathbf{x}_r), \quad (3.2) \quad \text{fun-2}$$

$$I_3(z) = 2\kappa^2 \operatorname{Im} \int_{\Gamma_r} \int_{\Gamma_s} \Phi_\kappa(\mathbf{z}, \mathbf{x}_r) \Phi_\kappa(\mathbf{z}, \mathbf{x}_s) \overline{M_{\mathbf{x}_r} u^{sc}(\mathbf{x}_r, \mathbf{x}_s)} \, ds(\mathbf{x}_s) ds(\mathbf{x}_r), \quad (3.3) \quad \text{fun-3}$$

$$I_4(z) = -2\kappa \operatorname{Re} \int_{\Gamma_r} \int_{\Gamma_s} \Phi_\kappa(\mathbf{z}, \mathbf{x}_r) \Phi_\kappa(\mathbf{z}, \mathbf{x}_s) \overline{N_{\mathbf{x}_r} u^{sc}(\mathbf{x}_r, \mathbf{x}_s)} \, ds(\mathbf{x}_s) ds(\mathbf{x}_r), \quad (3.4) \quad \text{fun-4}$$

$$I_5(z) = -\frac{\kappa^3}{4\pi} \operatorname{Im} \int_{\Gamma_r} \int_{\mathbb{S}} \Phi_\kappa(\mathbf{z}, \mathbf{x}_r) e^{i\kappa \mathbf{z} \cdot \mathbf{d}} \overline{u^{sc}(\mathbf{x}_r, \mathbf{d})} \, ds(\mathbf{d}) ds(\mathbf{x}_r), \quad (3.5) \quad \text{fun-5}$$

$$I_6(z) = -\frac{\kappa^2}{4\pi} \operatorname{Re} \int_{\Gamma_r} \int_{\mathbb{S}} \Phi_\kappa(\mathbf{z}, \mathbf{x}_r) e^{i\kappa \mathbf{z} \cdot \mathbf{d}} \overline{\partial_{\mathbf{n}(\mathbf{x}_r)} u^{sc}(\mathbf{x}_r, \mathbf{d})} \, ds(\mathbf{d}) ds(\mathbf{x}_r), \quad (3.6) \quad \text{fun-6}$$

$$I_7(z) = \frac{\kappa}{4\pi} \operatorname{Im} \int_{\Gamma_r} \int_{\mathbb{S}} \Phi_\kappa(\mathbf{z}, \mathbf{x}_r) e^{i\kappa \mathbf{z} \cdot \mathbf{d}} \overline{M_{\mathbf{x}_r} u^{sc}(\mathbf{x}_r, \mathbf{d})} \, ds(\mathbf{d}) ds(\mathbf{x}_r), \quad (3.7) \quad \text{fun-7}$$

$$I_8(z) = -\frac{1}{4\pi} \operatorname{Re} \int_{\Gamma_r} \int_{\mathbb{S}} \Phi_\kappa(\mathbf{z}, \mathbf{x}_r) e^{i\kappa \mathbf{z} \cdot \mathbf{d}} \overline{N_{\mathbf{x}_r} u^{sc}(\mathbf{x}_r, \mathbf{d})} \, ds(\mathbf{d}) ds(\mathbf{x}_r), \quad (3.8) \quad \text{fun-8}$$

$$I_9(z) = -\frac{\kappa^3}{4\pi} \operatorname{Im} \int_{\mathbb{S}} \int_{\Gamma_s} e^{-i\kappa \mathbf{z} \cdot \hat{\mathbf{x}}} \Phi_\kappa(\mathbf{z}, \mathbf{x}_s) \overline{u^\infty(\hat{\mathbf{x}}, \mathbf{x}_s)} \, ds(\mathbf{x}_s) ds(\hat{\mathbf{x}}), \quad (3.9) \quad \text{fun-9}$$

$$I_{10}(z) = -\frac{\kappa^2}{32\pi^2} \operatorname{Im} \int_{\mathbb{S}} \int_{\mathbb{S}} e^{i\kappa \mathbf{z} \cdot (\mathbf{d} - \hat{\mathbf{x}})} \overline{u^\infty(\hat{\mathbf{x}}, \mathbf{d})} \, ds(\mathbf{d}) ds(\hat{\mathbf{x}}). \quad (3.10) \quad \text{fun-10}$$

We start with some key lemmas that will occupy a central position in the rigorous analysis of our imaging functions.

asymptotic

Lemma 3.1 (see [5]).

$$\kappa \int_{\Gamma_r} \overline{\Phi_\kappa(\mathbf{x}, \mathbf{x}_r)} \Phi_\kappa(\mathbf{z}, \mathbf{x}_r) \, ds(\mathbf{x}_r) = \operatorname{Im} \Phi_\kappa(\mathbf{x}, \mathbf{z}) + w_{r,1}(\mathbf{x}, \mathbf{z}) \quad \forall \mathbf{x}, \mathbf{z} \in \Omega, \quad (3.11) \quad \text{eq:asy-1}$$

$$\kappa \int_{\Gamma_s} \overline{\Phi_\kappa(\mathbf{x}, \mathbf{x}_s)} \Phi_\kappa(\mathbf{z}, \mathbf{x}_s) ds(\mathbf{x}_r) = \text{Im } \Phi_\kappa(\mathbf{x}, \mathbf{z}) + w_{s,1}(\mathbf{x}, \mathbf{z}) \quad \forall \mathbf{x}, \mathbf{z} \in \Omega, \quad (3.12) \quad \text{eq:asy-2}$$

where $|\nabla_{\mathbf{x}}^3 w_{r,1}(\mathbf{x}, \mathbf{z})| \leq CR_r^{-1}$ and $|\nabla_{\mathbf{x}}^3 w_{s,1}(\mathbf{x}, \mathbf{z})| \leq CR_s^{-1}$ hold uniformly for any $\mathbf{x}, \mathbf{z} \in \Omega$. Here we employ the notation $|\nabla^3 v(\mathbf{x})| = \sum_{|\alpha|=0}^3 |\partial^{|\alpha|} v(\mathbf{x}) / \partial \mathbf{x}^\alpha|$.

Note that Lemma 3.1 is slightly different from Lemma 3.2 in [5], which is a direct consequence of the following asymptotic relation

$$\frac{\partial^{|\alpha|}}{\partial \mathbf{x}^\alpha} \Phi_\kappa(\mathbf{x}, \mathbf{x}_s) = O\left(R_s^{-1/2}\right), \quad |\alpha| = 0, 1, 2, 3, \quad (3.13) \quad \text{eq:highorder}$$

$$\frac{\partial^{|\alpha|}}{\partial \mathbf{x}^\alpha} (\partial_{r_s} \Phi_\kappa(\mathbf{x}, \mathbf{x}_s) - i\kappa \Phi_\kappa(\mathbf{x}, \mathbf{x}_s)) = O\left(R_s^{-3/2}\right), \quad |\alpha| = 0, 1, 2, 3 \quad (3.14) \quad \text{eq:highorder}$$

for any $\mathbf{x} \in \Omega$ and $\mathbf{x}_s \in \Gamma_s$.

Applying Lemma 3.1 could immediately yield the following result.

Lemma 3.2. *The following relation hold.*

$$-2\kappa^3 \int_{\Gamma_r} \overline{G(\mathbf{x}, \mathbf{x}_r)} \Phi_\kappa(\mathbf{z}, \mathbf{x}_r) ds(\mathbf{x}_r) = \text{Im } \Phi_\kappa(\mathbf{x}, \mathbf{z}) + w_{r,2}(\mathbf{x}, \mathbf{z}) \quad \forall \mathbf{x}, \mathbf{z} \in \Omega, \quad (3.15) \quad \text{eq:asy-3}$$

$$-2\kappa^2 \int_{\Gamma_r} \overline{\partial_{\mathbf{n}(\mathbf{x}_r)} G(\mathbf{x}, \mathbf{x}_r)} \Phi_\kappa(\mathbf{z}, \mathbf{x}_r) ds(\mathbf{x}_r) = -i (\text{Im } \Phi_\kappa(\mathbf{x}, \mathbf{z}) + w_{r,3}(\mathbf{x}, \mathbf{z})) \quad \forall \mathbf{x}, \mathbf{z} \in \Omega, \quad (3.16) \quad \text{eq:asy-4}$$

$$2\kappa \int_{\Gamma_r} \overline{M_{\mathbf{x}_r} G(\mathbf{x}, \mathbf{x}_r)} \Phi_\kappa(\mathbf{z}, \mathbf{x}_r) ds(\mathbf{x}_r) = \text{Im } \Phi_\kappa(\mathbf{x}, \mathbf{z}) + w_{r,4}(\mathbf{x}, \mathbf{z}) \quad \forall \mathbf{x}, \mathbf{z} \in \Omega, \quad (3.17) \quad \text{eq:asy-5}$$

$$2 \int_{\Gamma_r} \overline{N_{\mathbf{x}_r} G(\mathbf{x}, \mathbf{x}_r)} \Phi_\kappa(\mathbf{z}, \mathbf{x}_r) ds(\mathbf{x}_r) = i (\text{Im } \Phi_\kappa(\mathbf{x}, \mathbf{z}) + w_{r,5}(\mathbf{x}, \mathbf{z})) \quad \forall \mathbf{x}, \mathbf{z} \in \Omega, \quad (3.18) \quad \text{eq:asy-6}$$

where $|\nabla_{\mathbf{x}}^3 w_{r,j}(\mathbf{x}, \mathbf{z})| \leq CR_r^{-1}$ ($j = 2, 3, 4, 5$) hold uniformly for any $\mathbf{x}, \mathbf{z} \in \Omega$.

Proof. Note that

$$\begin{aligned} & -2\kappa^3 \int_{\Gamma_r} \overline{G(\mathbf{x}, \mathbf{x}_r)} \Phi_\kappa(\mathbf{z}, \mathbf{x}_r) ds(\mathbf{x}_r) \\ &= \kappa \int_{\Gamma_r} \overline{\Phi_\kappa(\mathbf{x}, \mathbf{x}_r)} \Phi_\kappa(\mathbf{z}, \mathbf{x}_r) ds(\mathbf{x}_r) - \kappa \int_{\Gamma_r} \overline{\Phi_{i\kappa}(\mathbf{x}, \mathbf{x}_r)} \Phi_\kappa(\mathbf{z}, \mathbf{x}_r) ds(\mathbf{x}_r). \end{aligned}$$

Using the following asymptotic behavior of the Hankel functions

$$H_m^{(1)}(it) = O\left(\frac{e^{-t}}{t^{1/2}}\right) \quad t \rightarrow +\infty, \quad m = 0, 1, \dots \quad (3.19) \quad \text{eq:antiHelmh}$$

and (3.11) in Lemma 3.1, we can prove (3.15). The estimate of $w_{r,2}$ follows from the estimate of $w_{r,1}$, (3.13) and the asymptotic behavior (3.19).

By the fact that Φ_κ satisfies the Sommerfeld radiation condition, we have that

$$\begin{aligned} & -2\kappa^2 \int_{\Gamma_r} \overline{\partial_{\mathbf{n}(\mathbf{x}_r)} G(\mathbf{x}, \mathbf{x}_r)} \Phi_\kappa(\mathbf{z}, \mathbf{x}_r) ds(\mathbf{x}_r) \\ &= \int_{\Gamma_r} \overline{\partial_{\mathbf{n}(\mathbf{x}_r)} \Phi_\kappa(\mathbf{x}, \mathbf{x}_r)} \Phi_\kappa(\mathbf{z}, \mathbf{x}_r) ds(\mathbf{x}_r) - \int_{\Gamma_r} \overline{\partial_{\mathbf{n}(\mathbf{x}_r)} \Phi_{i\kappa}(\mathbf{x}, \mathbf{x}_r)} \Phi_\kappa(\mathbf{z}, \mathbf{x}_r) ds(\mathbf{x}_r) \\ &= -i\kappa \int_{\Gamma_r} \overline{\Phi_\kappa(\mathbf{x}, \mathbf{x}_r)} \Phi_\kappa(\mathbf{z}, \mathbf{x}_r) ds(\mathbf{x}_r) + \int_{\Gamma_r} \overline{\partial_{\mathbf{n}(\mathbf{x}_r)} \Phi_\kappa(\mathbf{x}, \mathbf{x}_r) - i\kappa \Phi_\kappa(\mathbf{x}, \mathbf{x}_r)} \Phi_\kappa(\mathbf{z}, \mathbf{x}_r) ds(\mathbf{x}_r) \\ & \quad - \int_{\Gamma_r} \overline{\partial_{\mathbf{n}(\mathbf{x}_r)} \Phi_{i\kappa}(\mathbf{x}, \mathbf{x}_r)} \Phi_\kappa(\mathbf{z}, \mathbf{x}_r) ds(\mathbf{x}_r) = -i (\text{Im } \Phi_\kappa(\mathbf{x}, \mathbf{z}) + w_{r,3}(\mathbf{x}, \mathbf{z})), \end{aligned}$$

where we use [\(3.19\)](#). The estimate of $w_{r,3}$ can be obtained by the estimate of $w_{r,1}$, [\(3.14\)](#) and the asymptotic behavior [\(3.19\)](#).

Since Φ_κ (or $\Phi_{i\kappa}$) is the fundamental solution of Helmholtz equation with wave number κ (or $i\kappa$), we obtain

$$\begin{aligned}\Delta_{\mathbf{x}_r} G(\mathbf{x}, \mathbf{x}_r) &= \frac{1}{2\kappa^2} (\Delta_{\mathbf{x}_r} \Phi_{i\kappa}(\mathbf{x}, \mathbf{y}) - \Delta_{\mathbf{x}_r} \Phi_\kappa(\mathbf{x}, \mathbf{y})) \\ &= \frac{1}{2\kappa^2} (\kappa^2 \Phi_{i\kappa}(\mathbf{x}, \mathbf{y}) + \kappa^2 \Phi_\kappa(\mathbf{x}, \mathbf{y})) = \frac{1}{2} (\Phi_{i\kappa}(\mathbf{x}, \mathbf{y}) + \Phi_\kappa(\mathbf{x}, \mathbf{y})).\end{aligned}\tag{3.20} \quad \text{eq:laplace}$$

A substitution implies

$$\begin{aligned}& 2\kappa \int_{\Gamma_r} \overline{M_{\mathbf{x}_r} G(\mathbf{x}, \mathbf{x}_r)} \Phi_\kappa(\mathbf{z}, \mathbf{x}_r) \, ds(\mathbf{x}_r) \\ &= \kappa \int_{\Gamma_r} \left[\overline{\Phi_\kappa(\mathbf{x}, \mathbf{x}_r)} + \overline{\Phi_{i\kappa}(\mathbf{x}, \mathbf{x}_r)} + 2\overline{\mathcal{V}_1(\mathbf{x}, \mathbf{x}_r)} \right] \Phi_\kappa(\mathbf{z}, \mathbf{x}_r) \, ds(\mathbf{x}_r) \\ &= \text{Im } \Phi_\kappa(\mathbf{x}, \mathbf{z}) + w_{r,1}(\mathbf{x}, \mathbf{z}) + \kappa \int_{\Gamma_r} \overline{\Phi_{i\kappa}(\mathbf{x}, \mathbf{x}_r)} \Phi_\kappa(\mathbf{z}, \mathbf{x}_r) \, ds(\mathbf{x}_r) + 2\kappa \int_{\Gamma_r} \overline{\mathcal{V}_1(\mathbf{x}, \mathbf{x}_r)} \Phi_\kappa(\mathbf{z}, \mathbf{x}_r) \, ds(\mathbf{x}_r) \\ &= \text{Im } \Phi_\kappa(\mathbf{x}, \mathbf{z}) + w_{r,4}(\mathbf{x}, \mathbf{z}),\end{aligned}$$

where $\mathcal{V}_1(\mathbf{x}, \mathbf{x}_r) := M_{\mathbf{x}_r} G(\mathbf{x}, \mathbf{x}_r) - \Delta_{\mathbf{x}_r} G(\mathbf{x}, \mathbf{x}_r)$ and we use [\(3.11\)](#) and [\(2.12\)](#). The estimate of $w_{r,4}$ follows from the estimate of $w_{r,1}$ and the asymptotic behavior [\(3.19\)](#).

Analogously, by [\(2.13\)](#), [\(3.20\)](#) and [\(3.11\)](#), we have

$$\begin{aligned}& 2 \int_{\Gamma_r} \overline{N_{\mathbf{x}_r} G(\mathbf{x}, \mathbf{x}_r)} \Phi_\kappa(\mathbf{z}, \mathbf{x}_r) \, ds(\mathbf{x}_r) \\ &= - \int_{\Gamma_r} \left[\overline{\partial_{\mathbf{n}(\mathbf{x}_r)} \Phi_\kappa(\mathbf{x}, \mathbf{x}_r)} - \overline{\partial_{\mathbf{n}(\mathbf{x}_r)} \Phi_{i\kappa}(\mathbf{x}, \mathbf{x}_r)} + 2\overline{\mathcal{V}_2(\mathbf{x}, \mathbf{x}_r)} \right] \Phi_\kappa(\mathbf{z}, \mathbf{x}_r) \, ds(\mathbf{x}_r) \\ &= i\kappa \int_{\Gamma_r} \overline{\Phi_\kappa(\mathbf{x}, \mathbf{x}_r)} \Phi_\kappa(\mathbf{z}, \mathbf{x}_r) \, ds(\mathbf{x}_r) - \int_{\Gamma_r} \overline{\partial_{\mathbf{n}(\mathbf{x}_r)} \Phi_\kappa(\mathbf{x}, \mathbf{x}_r)} - i\kappa \overline{\Phi_\kappa(\mathbf{x}, \mathbf{x}_r)} \Phi_\kappa(\mathbf{z}, \mathbf{x}_r) \, ds(\mathbf{x}_r) \\ &\quad - \int_{\Gamma_r} \overline{\partial_{\mathbf{n}(\mathbf{x}_r)} \Phi_{i\kappa}(\mathbf{x}, \mathbf{x}_r)} \Phi_\kappa(\mathbf{z}, \mathbf{x}_r) \, ds(\mathbf{x}_r) + 2 \int_{\Gamma_r} \overline{\mathcal{V}_2(\mathbf{x}, \mathbf{x}_r)} \Phi_\kappa(\mathbf{z}, \mathbf{x}_r) \, ds(\mathbf{x}_r) \\ &= i (\text{Im } \Phi_\kappa(\mathbf{x}, \mathbf{z}) + w_{r,5}(\mathbf{x}, \mathbf{z})).\end{aligned}$$

where $\mathcal{V}_2(\mathbf{x}, \mathbf{x}_r) := N_{\mathbf{x}_r} G(\mathbf{x}, \mathbf{x}_r) + \partial_{\mathbf{n}(\mathbf{x}_r)} \Delta_{\mathbf{x}_r} G(\mathbf{x}, \mathbf{x}_r)$. The estimate of $w_{r,5}$ can be obtained by the estimate of $w_{r,1}$, [\(3.14\)](#) and the asymptotic behavior [\(3.19\)](#).

Therefore, the proof is complete. \square

We also need the following Funk-Hecke formula (c.f. [23, Lemma 2.7]) in our analysis.

lem:plane

Lemma 3.3. For any $\xi, \mathbf{z} \in \mathbb{R}^2$, we have

$$\int_{\mathbb{S}} e^{i\kappa \hat{\mathbf{x}} \cdot (\mathbf{z} - \xi)} \, ds(\hat{\mathbf{x}}) = 8\pi \text{Im } \Phi_\kappa(\xi, \mathbf{z}).\tag{3.21} \quad \text{eq:plane}$$

Now we are in a position to present the mathematical analysis of these imaging functions for extended obstacles in the following theorems.

Theorem 3.4. For any $\mathbf{z} \in \Omega$, it holds

$$I_j(\mathbf{z}) = \int_{\mathbb{S}} |\psi^\infty(\cdot, \mathbf{z})|^2 \, ds(\cdot) + w_j(\mathbf{z}) \quad \text{for } j = 1, 2, \dots, 10,$$

where $\psi^\infty(\cdot, \mathbf{z})$ is the far-field pattern of $\psi(\cdot, \mathbf{z})$, which is defined as the solution to the following boundary value problem:

$$\Delta_{\mathbf{x}}^2 \psi(\mathbf{x}, \mathbf{z}) - \kappa^4 \psi(\mathbf{x}, \mathbf{z}) = 0 \quad \text{in } D^c,$$

$$\begin{aligned} (\mathcal{B}_1\psi(\mathbf{x}, \mathbf{z}), \mathcal{B}_2\psi(\mathbf{x}, \mathbf{z})) &= -(\mathcal{B}_1\text{Im } \Phi(\mathbf{x}, \mathbf{z}), \mathcal{B}_2\text{Im } \Phi(\mathbf{x}, \mathbf{z})) \quad \text{on } \Gamma, \\ \partial_r\psi(\mathbf{x}, \mathbf{z}) - i\kappa\psi(\mathbf{x}, \mathbf{z}) &= o\left(\frac{1}{\sqrt{r}}\right) \quad r = |\mathbf{x}| \rightarrow \infty. \end{aligned}$$

Furthermore, the following inequalities hold

$$\begin{aligned} \|w_j\|_{L^\infty(\Omega)} &\leq C(R_r^{-1} + R_s^{-1}) \quad \text{for } j = 1, \dots, 4, \\ \|w_j\|_{L^\infty(\Omega)} &\leq CR_s^{-1} \quad \text{for } j = 5, \dots, 8, \quad \|w_9\|_{L^\infty(\Omega)} \leq CR_r^{-1}, \quad w_{10} = 0. \end{aligned}$$

Remark 3.5. The imaginary part of the fundamental solution $\text{Im } \Phi_\kappa(\xi, \mathbf{z})$, i.e., the Bessel function of order zero, attains the largest value when \mathbf{z} is equal to ξ and has small values when \mathbf{z} is far from ξ . However, $\partial_{\mathbf{n}(\xi)}\text{Im } \Phi_\kappa(\xi, \mathbf{z})$ can attain larger value when \mathbf{z} is near ξ and has small values when \mathbf{z} is far from ξ . Note that $\psi(\xi, \mathbf{z})$ is the solution to $(2.5a)-(2.5c)$ with boundary data $(f, g) = -(\text{Im } \Phi_\kappa(\xi, \mathbf{z}), \partial_{\mathbf{n}(\xi)}\text{Im } \Phi_\kappa(\xi, \mathbf{z}))$. Therefore, the imaging functions $I_j(\mathbf{z})$ ($j = 1, 2, \dots, 10$) will exhibit a distinct contrast near the boundary Γ of the scatterer D and decay with distance from the boundary Γ , which will be confirmed in the numerical examples in Section 5. sec: numerical

Proof. We will present the proof of the cases of boundary conditions I and II. The cases of boundary conditions III and IV can be treated similarly and to avoid repetition, we omit the proof.

Proof of the case of boundary condition I.

The proof is divided into five cases.

Case 1: $j = 1$ and 5 . eq: Green-rep

Applying (2.9) in Lemma 2.2 to $w(\xi) = u^{sc}(\xi, \mathbf{x}_s)$ ($\mathbf{x}_s \in \Gamma_s$) or $u^{sc}(\xi, \mathbf{d})$ ($\mathbf{d} \in \mathbb{S}$) could yield lem: rep

$$\begin{aligned} w(\mathbf{x}_r) &= \int_{\partial D} \left\{ [G(\xi, \mathbf{x}_r) N_\xi w(\xi) + \partial_{\mathbf{n}(\xi)} G(\xi, \mathbf{x}_r) M_\xi w(\xi)] \right. \\ &\quad \left. - [N_\xi G(\xi, \mathbf{x}_r) w(\xi) + M_\xi G(\xi, \mathbf{x}_r) \partial_{\mathbf{n}(\xi)} w(\xi)] \right\} ds(\xi) \quad \mathbf{x}_r \in \Gamma_r. \end{aligned} \quad (3.23) \quad \text{eq: eq:Green-}$$

Then exchanging the order of integration and using (3.15) in Lemma 3.2, we obtain eq: asy-3 lem: asymptotic-2

$$\begin{aligned} &- 2\kappa^3 \int_{\Gamma_r} \Phi_\kappa(\mathbf{z}, \mathbf{x}_r) \overline{w(\mathbf{x}_r)} ds(\mathbf{x}_r) \\ &= \int_\Gamma \left\{ [M_\xi \overline{w(\xi)} \partial_{\mathbf{n}(\xi)} (\text{Im } \Phi_\kappa(\xi, \mathbf{z}) + w_{r,2}(\xi, \mathbf{z})) + N_\xi \overline{w(\xi)} (\text{Im } \Phi_\kappa(\xi, \mathbf{z}) + w_{r,2}(\xi, \mathbf{z}))] \right. \\ &\quad \left. - [\partial_{\mathbf{n}(\xi)} \overline{w(\xi)} M_\xi (\text{Im } \Phi_\kappa(\xi, \mathbf{z}) + w_{r,2}(\xi, \mathbf{z})) + \overline{w(\xi)} N_\xi (\text{Im } \Phi_\kappa(\xi, \mathbf{z}) + w_{r,2}(\xi, \mathbf{z}))] \right\} ds(\xi). \end{aligned}$$

Define

$$v_s(\xi, \mathbf{z}) = \kappa \int_{\Gamma_s} \Phi_\kappa(\mathbf{z}, \mathbf{x}_s) \overline{u^{sc}(\xi, \mathbf{x}_s)} ds(\mathbf{x}_s) \quad \text{and} \quad v_d(\xi, \mathbf{z}) = \frac{1}{8\pi} \int_{\Gamma_s} e^{i\kappa \mathbf{z} \cdot \mathbf{d}} \overline{u^{sc}(\xi, \mathbf{d})} ds(\mathbf{d}). \quad (3.24) \quad \text{eq: vsd}$$

The imaging functions $I_j(\mathbf{z})$ ($j = 1, 5$) can be rewritten as follows:

$$\begin{aligned} I_j(\mathbf{z}) &= \text{Im} \int_\Gamma \left\{ [M \cdot \overline{v(\cdot)} \partial_{\mathbf{n}(\cdot)} (\text{Im } \Phi_\kappa(\cdot, \mathbf{z}) + w_{r,2}(\cdot, \mathbf{z})) + N \cdot \overline{v(\cdot)} (\text{Im } \Phi_\kappa(\cdot, \mathbf{z}) + w_{r,2}(\cdot, \mathbf{z}))] \right. \\ &\quad \left. - [\partial_{\mathbf{n}(\cdot)} \overline{v(\cdot)} M \cdot (\text{Im } \Phi_\kappa(\cdot, \mathbf{z}) + w_{r,2}(\cdot, \mathbf{z})) + \overline{v(\cdot)} N \cdot (\text{Im } \Phi_\kappa(\cdot, \mathbf{z}) + w_{r,2}(\cdot, \mathbf{z}))] \right\} ds(\cdot), \end{aligned} \quad (3.25) \quad \text{eq: imaging}$$

where we set $v(\xi) = v_s(\xi, \mathbf{z})$ or $v_d(\xi, \mathbf{z})$ for brevity.

Next, we claim that

$$v_s(\xi, \mathbf{z}) = \overline{\psi(\xi, \mathbf{z})} + \overline{\zeta(\xi, \mathbf{z})} \quad \text{and} \quad v_d(\xi, \mathbf{z}) = \overline{\psi(\xi, \mathbf{z})}, \quad (3.26) \quad \text{eq: decomposi}$$

where $\zeta(\cdot, \mathbf{z})$ is a solution of [\(2.5a\)-\(2.5c\)](#) with $f = -w_s(\cdot, \mathbf{z})$ and $g = -\partial_{\mathbf{n}(\cdot)} w_s(\cdot, \mathbf{z})$. It follows from [Lemma 2.1](#) that

$$\|\zeta(\cdot, \mathbf{z})\|_{H^{3/2}(\Gamma)} + \|\partial_{\mathbf{n}(\cdot)} \zeta(\cdot, \mathbf{z})\|_{H^{1/2}(\Gamma)} + \|M\zeta(\cdot, \mathbf{z})\|_{H^{-1/2}(\Gamma)} + \|N\zeta(\cdot, \mathbf{z})\|_{H^{-3/2}(\Gamma)} \leq CR_s^{-1} \quad (3.27) \quad \text{eq:zeta}$$

holds uniformly for any $\mathbf{z} \in \Omega$.

We note that the scattered field u^{sc} satisfies [\(2.1\)](#) and [\(2.3\)](#), which implies that the complex conjugate $\overline{v(\xi)}$ also satisfies the biharmonic wave equation [\(2.1\)](#), i.e.,

$$\Delta_\xi^2 \overline{v(\xi)} - \kappa^4 \overline{v(\xi)} = 0 \quad \text{in } D^c,$$

and the Sommerfeld radiation condition [\(2.3\)](#). By the boundary conditions [\(2.2\)](#) and [Lemma 3.1](#), we have

$$\begin{aligned} \overline{v_s(\xi, \mathbf{z})} &= \kappa \int_{\Gamma_s} \overline{\Phi_\kappa(\mathbf{z}, \mathbf{x}_s)} u^{sc}(\xi, \mathbf{x}_s) \, ds(\mathbf{x}_s) \\ &= -\kappa \int_{\Gamma_s} \overline{\Phi_\kappa(\mathbf{z}, \mathbf{x}_s)} \Phi_\kappa(\xi, \mathbf{x}_s) \, ds(\mathbf{x}_s) = -(\text{Im } \Phi_\kappa(\xi, \mathbf{z}) + w_{s,1}(\xi, \mathbf{z})) \quad \xi \in \Gamma, \\ \partial_{\mathbf{n}(\xi)} \overline{v_s(\xi, \mathbf{z})} &= \kappa \int_{\Gamma_s} \overline{\Phi_\kappa(\mathbf{z}, \mathbf{x}_s)} \partial_{\mathbf{n}(\xi)} u^{sc}(\xi, \mathbf{x}_s) \, ds(\mathbf{x}_s) \\ &= -\kappa \int_{\Gamma_s} \overline{\Phi_\kappa(\mathbf{z}, \mathbf{x}_s)} \partial_{\mathbf{n}(\xi)} \Phi_\kappa(\xi, \mathbf{x}_s) \, ds(\mathbf{x}_s) = -\partial_{\mathbf{n}(\xi)} (\text{Im } \Phi_\kappa(\xi, \mathbf{z}) + w_{s,1}(\xi, \mathbf{z})) \quad \xi \in \Gamma. \end{aligned}$$

Alternatively, from [Lemma 3.3](#) we conclude that

$$\begin{aligned} \overline{v_d(\xi, \mathbf{z})} &= \frac{1}{8\pi} \int_{\mathbb{S}} e^{i\kappa \mathbf{z} \cdot \mathbf{d}} u^{sc}(\xi, \mathbf{d}) \, ds(\mathbf{d}) = -\frac{1}{8\pi} \int_{\mathbb{S}} e^{i\kappa(\xi - \mathbf{z}) \cdot \mathbf{d}} \, ds(\mathbf{d}) = -\text{Im } \Phi_\kappa(\xi, \mathbf{z}) \quad \xi \in \Gamma, \\ \partial_{\mathbf{n}(\xi)} \overline{v_d(\xi, \mathbf{z})} &= \frac{1}{8\pi} \int_{\mathbb{S}} e^{i\kappa \mathbf{z} \cdot \mathbf{d}} \partial_{\mathbf{n}(\xi)} u^{sc}(\xi, \mathbf{d}) \, ds(\mathbf{d}) \\ &= -\frac{1}{8\pi} \partial_{\mathbf{n}(\xi)} \int_{\mathbb{S}} e^{i\kappa(\xi - \mathbf{z}) \cdot \mathbf{d}} \, ds(\mathbf{d}) = -\partial_{\mathbf{n}(\xi)} \text{Im } \Phi_\kappa(\xi, \mathbf{z}) \quad \xi \in \Gamma. \end{aligned}$$

Hence, the well-posedness of the direct problem, i.e., [Theorem 2.1](#), shows that [\(3.25\)](#) $\overline{v_s(\xi, \mathbf{z})} = \psi(\xi, \mathbf{z}) + \zeta(\xi, \mathbf{z})$ and $\overline{v_d(\xi, \mathbf{z})} = \psi(\xi, \mathbf{z})$, which immediately leads to the decomposition [\(3.26\)](#).

Substituting the decomposition [\(3.26\)](#) into [\(3.25\)](#), we find that

$$\begin{aligned} I_j(\mathbf{z}) &= \text{Im} \int_{\Gamma} \left\{ [M_\xi \overline{\psi(\xi, \mathbf{z})} \partial_{\mathbf{n}(\xi)} (\text{Im } \Phi_\kappa(\xi, \mathbf{z})) + N_\xi \overline{\psi(\xi, \mathbf{z})} (\text{Im } \Phi_\kappa(\xi, \mathbf{z}))] \right. \\ &\quad \left. - [\partial_{\mathbf{n}(\xi)} \overline{\psi(\xi, \mathbf{z})} M_\xi (\text{Im } \Phi_\kappa(\xi, \mathbf{z})) + \overline{\psi(\xi, \mathbf{z})} N_\xi (\text{Im } \Phi_\kappa(\xi, \mathbf{z}))] \right\} ds(\xi) + w_j, \quad (3.28) \quad \text{eq:imaging-1} \end{aligned}$$

for $j = 1, 5$. Here $\|w_1\|_{L^\infty(\Omega)} \leq C(R_r^{-1} + R_s^{-1})$ and $\|w_5\|_{L^\infty(\Omega)} \leq CR_s^{-1}$. Since $\psi(\xi, \mathbf{z})$ satisfies the clamped plate boundary condition, i.e.,

$$\psi(\xi, \mathbf{z}) = -\text{Im } \Phi_\kappa(\xi, \mathbf{z}) \quad \text{and} \quad \partial_{\mathbf{n}(\xi)} \psi(\xi, \mathbf{z}) = -\partial_{\mathbf{n}(\xi)} \text{Im } \Phi_\kappa(\xi, \mathbf{z}) \quad \xi \in \Gamma,$$

applying integration by parts yields

$$\begin{aligned} &\text{Im} \int_{\Gamma} [\partial_{\mathbf{n}(\xi)} \overline{\psi(\xi, \mathbf{z})} M_\xi (\text{Im } \Phi_\kappa(\xi, \mathbf{z})) + \overline{\psi(\xi, \mathbf{z})} N_\xi (\text{Im } \Phi_\kappa(\xi, \mathbf{z}))] ds(\xi) \\ &= -\text{Im} \int_{\Gamma} [\partial_{\mathbf{n}(\xi)} \text{Im } \Phi_\kappa(\xi, \mathbf{z}) M_\xi (\text{Im } \Phi_\kappa(\xi, \mathbf{z})) + \text{Im } \Phi_\kappa(\xi, \mathbf{z}) N_\xi (\text{Im } \Phi_\kappa(\xi, \mathbf{z}))] ds(\xi) \\ &= -\text{Im} \int_D [|\Delta_\xi (\text{Im } \Phi_\kappa(\xi, \mathbf{z}))|^2 - \kappa^4 |\text{Im } \Phi_\kappa(\xi, \mathbf{z})|^2] d\xi = 0, \end{aligned}$$

which leads to

$$\begin{aligned}
I_j(\mathbf{z}) &= \text{Im} \int_{\Gamma} [M_{\xi} \overline{\psi(\xi, \mathbf{z})} \partial_{\mathbf{n}(\xi)} (\text{Im} \Phi_{\kappa}(\xi, \mathbf{z})) + N_{\xi} \overline{\psi(\xi, \mathbf{z})} (\text{Im} \Phi_{\kappa}(\xi, \mathbf{z}))] \, ds(\xi) + w_j \\
&= - \text{Im} \int_{\Gamma} [M_{\xi} \overline{\psi(\xi, \mathbf{z})} \partial_{\mathbf{n}(\xi)} \psi(\xi, \mathbf{z}) + N_{\xi} \overline{\psi(\xi, \mathbf{z})} \psi(\xi, \mathbf{z})] \, ds(\xi) + w_j \\
&= \frac{\kappa^2}{4\pi} \int_{\mathbb{S}} |\psi^{\infty}(\cdot, \mathbf{z})|^2 \, ds(\cdot) + w_j \quad \text{for } j = 1, 5,
\end{aligned}$$

where we use Lemma [2.3](#) ^{[lem:sign](#)}.

Case 2: $j = 2$ and 6 .

First, using the definitions of $v_s(\xi, \mathbf{z})$ and $v_d(\xi, \mathbf{d})$ in [\(3.24\)](#) ^{[eq:vsd](#)}, we show that for $\mathbf{z} \in \Omega$ and $j = 2, 6$, it holds that

$$\begin{aligned}
I_j(\mathbf{z}) &= \text{Im} \int_{\Gamma} \left\{ [M \cdot \overline{v(\cdot)} \partial_{\mathbf{n}(\cdot)} (\text{Im} \Phi_{\kappa}(\cdot, \mathbf{z}) + w_{r,3}(\cdot, \mathbf{z})) + N \cdot \overline{v(\cdot)} (\text{Im} \Phi_{\kappa}(\cdot, \mathbf{z}) + w_{r,3}(\cdot, \mathbf{z}))] \right. \\
&\quad \left. - [\partial_{\mathbf{n}(\cdot)} \overline{v(\cdot)} M \cdot (\text{Im} \Phi_{\kappa}(\cdot, \mathbf{z}) + w_{r,3}(\cdot, \mathbf{z})) + \overline{v(\cdot)} N \cdot (\text{Im} \Phi_{\kappa}(\cdot, \mathbf{z}) + w_{r,3}(\cdot, \mathbf{z}))] \right\} \, ds(\cdot), \quad (3.29)
\end{aligned}$$

[eq:imaging-2](#)

where $v(\xi) = v_s(\xi, \mathbf{z})$ when $j = 2$ or $v(\xi) = v_d(\xi, \mathbf{d})$ when $j = 6$.

Recalling the representation [\(2.9\)](#) in Lemma [2.2](#) ^{[eq:green-rep](#)} and considering the normal derivative of $w(\xi) = u^{sc}(\xi, \mathbf{x}_s)$ ($\mathbf{x}_s \in \Gamma_s$) or $u^{sc}(\xi, \mathbf{d})$ ($\mathbf{d} \in \mathbb{S}$), we find that

$$\begin{aligned}
\partial_{\mathbf{n}(\mathbf{x}_r)} w(\mathbf{x}_r) &= \int_{\partial D} \left\{ [\partial_{\mathbf{n}(\mathbf{x}_r)} G(\xi, \mathbf{x}_r) N_{\xi} w(\xi) + \partial_{\mathbf{n}(\xi)} \partial_{\mathbf{n}(\mathbf{x}_r)} G(\xi, \mathbf{x}_r) M_{\xi} w(\xi)] \right. \\
&\quad \left. - [N_{\xi} \partial_{\mathbf{n}(\mathbf{x}_r)} G(\xi, \mathbf{x}_r) w(\xi) + M_{\xi} \partial_{\mathbf{n}(\mathbf{x}_r)} G(\xi, \mathbf{x}_r) \partial_{\mathbf{n}(\xi)} w(\xi)] \right\} \, ds(\xi) \quad \mathbf{x}_r \in \Gamma_r.
\end{aligned}$$

In view of [\(3.12\)](#) in Lemma [3.2](#) ^{[eq:asy-2](#)} one has [lem:asymptotic-2](#)

$$\begin{aligned}
&- 2\kappa^2 \int_{\Gamma_r} \Phi_{\kappa}(\mathbf{z}, \mathbf{x}_r) \overline{\partial_{\mathbf{n}(\mathbf{x}_r)} w(\mathbf{x}_r)} \, ds(\mathbf{x}_r) \\
&= -i \int_{\Gamma} \left\{ [M_{\xi} \overline{w(\xi)} \partial_{\mathbf{n}(\xi)} (\text{Im} \Phi_{\kappa}(\xi, \mathbf{z}) + w_{r,3}(\xi, \mathbf{z})) + N_{\xi} \overline{w(\xi)} (\text{Im} \Phi_{\kappa}(\xi, \mathbf{z}) + w_{r,3}(\xi, \mathbf{z}))] \right. \\
&\quad \left. - [\partial_{\mathbf{n}(\xi)} \overline{w(\xi)} M_{\xi} (\text{Im} \Phi_{\kappa}(\xi, \mathbf{z}) + w_{r,3}(\xi, \mathbf{z})) + \overline{w(\xi)} N_{\xi} (\text{Im} \Phi_{\kappa}(\xi, \mathbf{z}) + w_{r,3}(\xi, \mathbf{z}))] \right\} \, ds(\xi).
\end{aligned}$$

Similarly, combining a substitution and the definitions of function v and imaging functions I_j ($j = 3, 7$), we can obtain [\(3.29\)](#) ^{[eq:imaging-2](#)}, where we use the fact that $\text{Re}(-ic) = \text{Im} c$ for any complex number $c \in \mathbb{C}$.

Next, the decomposition of v , i.e., [\(3.26\)](#) ^{[eq:decomposition](#)} and [\(3.29\)](#) ^{[eq:imaging-1](#)} can give [\(3.28\)](#) with w_1 (or w_5) replaced by w_2 (or w_6). Proceeding as in case 1 immediately can prove the conclusion.

Case 3: $j = 3$ and 7 .

It remains to prove [\(3.29\)](#) ^{[eq:imaging-2](#)} with $w_{r,3}$ replaced by $w_{r,4}$. It follows from the representation [\(2.9\)](#) ^{[eq:green-rep](#)} in Lemma [2.2](#) ^{[lem:rep](#)} that

$$\begin{aligned}
M_{\mathbf{x}_r} w(\mathbf{x}_r) &= \int_{\partial D} \left\{ [M_{\mathbf{x}_r} G(\xi, \mathbf{x}_r) N_{\xi} w(\xi) + \partial_{\mathbf{n}(\xi)} M_{\mathbf{x}_r} G(\xi, \mathbf{x}_r) M_{\xi} w(\xi)] \right. \\
&\quad \left. - [N_{\xi} M_{\mathbf{x}_r} G(\xi, \mathbf{x}_r) w(\xi) + M_{\xi} M_{\mathbf{x}_r} G(\xi, \mathbf{x}_r) \partial_{\mathbf{n}(\xi)} w(\xi)] \right\} \, ds(\xi) \quad \mathbf{x}_r \in \Gamma_r,
\end{aligned}$$

where $w(\xi)$ is $u^{sc}(\xi, \mathbf{x}_s)$ or $u^{sc}(\xi, \mathbf{d})$. Using [\(3.17\)](#) in Lemma [3.2](#) ^{[eq:asy-5](#)} ^{[lem:asymptotic-2](#)}, we get

$$\begin{aligned}
&2\kappa \int_{\Gamma_r} \Phi_{\kappa}(\mathbf{z}, \mathbf{x}_r) \overline{M_{\mathbf{x}_r} w(\mathbf{x}_r)} \, ds(\mathbf{x}_r) \\
&= \int_{\Gamma} \left\{ [M_{\xi} \overline{w(\xi)} \partial_{\mathbf{n}(\xi)} (\text{Im} \Phi_{\kappa}(\xi, \mathbf{z}) + w_{r,4}(\xi, \mathbf{z})) + N_{\xi} \overline{w(\xi)} (\text{Im} \Phi_{\kappa}(\xi, \mathbf{z}) + w_{r,4}(\xi, \mathbf{z}))] \right.
\end{aligned}$$

$$- [\partial_{\mathbf{n}(\xi)} \overline{w(\xi)} M_\xi (\text{Im } \Phi_\kappa(\xi, \mathbf{z}) + w_{r,4}(\xi, \mathbf{z})) + \overline{w(\xi)} N_\xi (\text{Im } \Phi_\kappa(\xi, \mathbf{z}) + w_{r,4}(\xi, \mathbf{z}))] \} ds(\xi),$$

which proves (3.29) with $w_{r,3}$ replaced by $w_{r,4}$ due to the definitions of function v and imaging functions I_j ($j = 3, 7$).

Case 4: $j = 4$ and 8.

It remains to prove (3.29) with $w_{r,3}$ replaced by $w_{r,5}$. Using the representation (2.9) in Lemma 2.2, we see that

$$N_{\mathbf{x}_r} w(\mathbf{x}_r) = \int_{\partial D} \left\{ [N_{\mathbf{x}_r} G(\xi, \mathbf{x}_r) N_\xi w(\xi) + \partial_{\mathbf{n}(\xi)} N_{\mathbf{x}_r} G(\xi, \mathbf{x}_r) M_\xi w(\xi)] \right. \\ \left. - [N_\xi N_{\mathbf{x}_r} G(\xi, \mathbf{x}_r) w(\xi) + M_\xi N_{\mathbf{x}_r} G(\xi, \mathbf{x}_r) \partial_{\mathbf{n}(\xi)} w(\xi)] \right\} ds(\xi),$$

where $\mathbf{x}_r \in \Gamma_r$ and $w(\xi)$ is $u^{sc}(\xi, \mathbf{x}_s)$ or $u^{sc}(\xi, \mathbf{d})$. Then we employ (3.18) in Lemma 3.2 to get

$$- 2\kappa \int_{\Gamma_r} \Phi_\kappa(\mathbf{z}, \mathbf{x}_r) \overline{N_{\mathbf{x}_r} w(\mathbf{x}_r)} ds(\mathbf{x}_r) \\ = -i \int_{\Gamma} \left\{ [M_\xi \overline{w(\xi)} \partial_{\mathbf{n}(\xi)} (\text{Im } \Phi_\kappa(\xi, \mathbf{z}) + w_{r,5}(\xi, \mathbf{z})) + N_\xi \overline{w(\xi)} (\text{Im } \Phi_\kappa(\xi, \mathbf{z}) + w_{r,5}(\xi, \mathbf{z}))] \right. \\ \left. - [\partial_{\mathbf{n}(\xi)} \overline{w(\xi)} M_\xi (\text{Im } \Phi_\kappa(\xi, \mathbf{z}) + w_{r,5}(\xi, \mathbf{z})) - \overline{w(\xi)} N_\xi (\text{Im } \Phi_\kappa(\xi, \mathbf{z}) + w_{r,5}(\xi, \mathbf{z}))] \right\} ds(\xi).$$

By means of this, (3.24) and the fact that $\text{Re}(-ic) = \text{Im} c$ for $c \in \mathbb{C}$, the imaging functions I_j ($j = 4, 8$) can be transformed into (3.29) with $w_{r,3}$ replaced by $w_{r,5}$.

Case 5: $j = 5$ and 10.

It remains to prove (3.29) with $w_{r,3}$ replaced by 0. By (2.10) in Lemma 2.2, the far-field pattern w^∞ of w is given by

$$w^\infty(\hat{\mathbf{x}}) = -\frac{1}{2\kappa^2} \int_{\Gamma} \left\{ [e^{-i\kappa \hat{\mathbf{x}} \cdot \xi} N_\xi w(\xi) + \partial_{\mathbf{n}(\xi)} e^{-i\kappa \hat{\mathbf{x}} \cdot \xi} M_\xi w(\xi)] \right. \\ \left. - [N_\xi e^{-i\kappa \hat{\mathbf{x}} \cdot \xi} w(\xi) + M_\xi e^{-i\kappa \hat{\mathbf{x}} \cdot \xi} \partial_{\mathbf{n}(\xi)} w(\xi)] \right\} ds(\xi) \quad \hat{\mathbf{x}} \in \mathbb{S},$$

where $w(\xi)$ denotes $u^{sc}(\xi, \mathbf{x}_s)$ or $u^{sc}(\xi, \mathbf{d})$. From Lemma 3.3, we observe that

$$\frac{-2\kappa^2}{8\pi} \int_{\mathbb{S}} e^{-i\kappa \hat{\mathbf{x}} \cdot \mathbf{z}} \overline{w^\infty(\hat{\mathbf{x}})} ds(\hat{\mathbf{x}}) \\ = \int_{\Gamma} \left\{ [M_\xi \overline{w(\xi)} \partial_{\mathbf{n}(\xi)} \left(\frac{1}{8\pi} \int_{\mathbb{S}} e^{i\kappa \hat{\mathbf{x}} \cdot (\xi - \mathbf{z})} ds(\hat{\mathbf{x}}) \right) + N_\xi \overline{w(\xi)} \left(\frac{1}{8\pi} \int_{\mathbb{S}} e^{i\kappa \hat{\mathbf{x}} \cdot (\xi - \mathbf{z})} ds(\hat{\mathbf{x}}) \right)] \right. \\ \left. - [\partial_{\mathbf{n}(\xi)} \overline{w(\xi)} M_\xi \left(\frac{1}{8\pi} \int_{\mathbb{S}} e^{i\kappa \hat{\mathbf{x}} \cdot (\xi - \mathbf{z})} ds(\hat{\mathbf{x}}) \right) + \overline{w(\xi)} N_\xi \left(\frac{1}{8\pi} \int_{\mathbb{S}} e^{i\kappa \hat{\mathbf{x}} \cdot (\xi - \mathbf{z})} ds(\hat{\mathbf{x}}) \right)] \right\} ds(\xi) \\ = \int_{\Gamma} \left\{ [M_\xi \overline{w(\xi)} \partial_{\mathbf{n}(\xi)} (\text{Im } \Phi_\kappa(\xi, \mathbf{z})) + N_\xi \overline{w(\xi)} (\text{Im } \Phi_\kappa(\xi, \mathbf{z}))] \right. \\ \left. - [\partial_{\mathbf{n}(\xi)} \overline{w(\xi)} M_\xi (\text{Im } \Phi_\kappa(\xi, \mathbf{z})) + \overline{w(\xi)} N_\xi (\text{Im } \Phi_\kappa(\xi, \mathbf{z}))] \right\} ds(\xi).$$

Then combinations of (3.24), (3.9) and (3.10) leads to (3.29) with $w_{r,3}$ replaced by 0.

Proof of the case of boundary condition II.

By the arguments in the proof of the case of the boundary condition I, we obtain

$$I_j(\mathbf{z}) = \text{Im} \int_{\Gamma} \left\{ [M_\xi \overline{\psi(\xi, \mathbf{z})} \partial_{\mathbf{n}(\xi)} (\text{Im } \Phi_\kappa(\xi, \mathbf{z})) + N_\xi \overline{\psi(\xi, \mathbf{z})} (\text{Im } \Phi_\kappa(\xi, \mathbf{z}))] \right. \\ \left. - [\partial_{\mathbf{n}(\xi)} \overline{\psi(\xi, \mathbf{z})} M_\xi (\text{Im } \Phi_\kappa(\xi, \mathbf{z})) + \overline{\psi(\xi, \mathbf{z})} N_\xi (\text{Im } \Phi_\kappa(\xi, \mathbf{z}))] \right\} ds(\xi) + w_j \quad j = 1, 2, \dots, 10.$$

Obviously, the function $\psi(\xi, \mathbf{z})$ in the case satisfies the simply supported boundary condition, i.e.,

$$\psi(\xi, \mathbf{z}) = -\text{Im } \Phi_\kappa(\xi, \mathbf{z}) \quad \text{and} \quad M_{\mathbf{n}(\xi)}\psi(\xi, \mathbf{z}) = -M_\xi \text{Im } \Phi_\kappa(\xi, \mathbf{z}) \quad \xi \in \Gamma,$$

which leads to

$$\begin{aligned} & \text{Im} \int_\Gamma [M_\xi \overline{\psi(\xi, \mathbf{z})} \partial_{\mathbf{n}(\xi)}(\text{Im } \Phi_\kappa(\xi, \mathbf{z})) - \overline{\psi(\xi, \mathbf{z})} N_\xi(\text{Im } \Phi_\kappa(\xi, \mathbf{z}))] ds(\xi) \\ &= -\text{Im} \int_\Gamma [M_\xi \text{Im } \Phi_\kappa(\xi, \mathbf{z}) \partial_{\mathbf{n}(\xi)}(\text{Im } \Phi_\kappa(\xi, \mathbf{z})) - \text{Im } \Phi_\kappa(\xi, \mathbf{z}) N_\xi(\text{Im } \Phi_\kappa(\xi, \mathbf{z}))] ds(\xi) = 0. \end{aligned}$$

Hence we arrive at

$$\begin{aligned} I_j(\mathbf{z}) &= \text{Im} \int_\Gamma \left\{ N_\xi \overline{\psi(\xi, \mathbf{z})} (\text{Im } \Phi_\kappa(\xi, \mathbf{z})) \right\} - \partial_{\mathbf{n}(\xi)} \overline{\psi(\xi, \mathbf{z})} M_\xi (\text{Im } \Phi_\kappa(\xi, \mathbf{z})) \Big\} ds(\xi) + w_j \\ &= -\text{Im} \int_\Gamma \left\{ \psi(\xi, \mathbf{z}) N_\xi \overline{\psi(\xi, \mathbf{z})} - \partial_{\mathbf{n}(\xi)} \overline{\psi(\xi, \mathbf{z})} M_\xi (\psi(\xi, \mathbf{z})) \right\} ds(\xi) + w_j \\ &= \frac{\kappa^2}{4\pi} \int_S |\psi^\infty(\cdot, \mathbf{z})|^2 ds(\cdot) + w_j \quad \text{for } j = 1, 2, \dots, 10, \end{aligned}$$

where we use Lemma [2.3](#). [lem:sign](#) This allows us to conclude the proof. □

We end this section by the following reconstruction algorithm:

Reconstruction algorithm for extended obstacles with phased data

- Choose a sampling domain Ω and generate sampling points.
- For each sampling point $\mathbf{z} \in \Omega$, calculate the imaging function $I_j(\mathbf{z})$ for $j = 1, 2, \dots, 10$.
- Plot the contours for the imaging functions

$$\hat{I}_j(\mathbf{z}) = \frac{I_j(\mathbf{z})}{\max_{\mathbf{z} \in \Omega} I_j(\mathbf{z})} \quad j = 1, 2, \dots, 10.$$

4 The direct imaging method with phaseless data

rec:phaseless

In this section, we develop the direct imaging method with phaseless data. To this end, we introduce the following imaging function for **IP-11**.

$$I_{11}(\mathbf{z}) = -2\kappa^4 \text{Im} \int_{\Gamma_r} \int_{\Gamma_s} \Phi_\kappa(\mathbf{z}, \mathbf{x}_r) \Phi_\kappa(\mathbf{z}, \mathbf{x}_s) \frac{|u(\mathbf{x}_r, \mathbf{x}_s)|^2 - |\Phi_\kappa(\mathbf{x}_r, \mathbf{x}_s)|^2}{\Phi_\kappa(\mathbf{x}_r, \mathbf{x}_s)} ds(\mathbf{x}_s) ds(\mathbf{x}_r) \quad \mathbf{z} \in \Omega.$$

Without loss of generality, assume $R_r = \tau R_s$ with $\tau \geq 1$. First, we start with some lemmas.

Lemma 4.1. *There exists a constant $C > 0$ such that*

$$|u^{sc}(\mathbf{x}_r, \mathbf{x}_s)| \leq C R_r^{-1/2} R_s^{-1/2} \quad \text{for } \mathbf{x}_r \in \Gamma_r, \mathbf{x}_s \in \Gamma_s,$$

where the constant C depends on the wave number κ and the domain D .

Proof. The proof is a direct consequence of the representation [\(2.9\)](#) in [lem:Green-rep](#) Lemma [2.2](#), [lem:rep](#) Lemma [2.1](#) and the following estimate of Hankel functions (see [\[8, \(3.8\)\]](#))

$$|H_0^{(1)}(t)| \leq \left(\frac{2}{\pi t}\right)^{1/2}, \quad |H_1^{(1)}(t)| \leq \left(\frac{2}{\pi t}\right)^{1/2} + \frac{2}{\pi t} \quad \text{for } t > 0.$$

□

Lemma 4.2 (see [12]). *It holds that*

$$u^\infty(-\mathbf{d}, \mathbf{x}) = \frac{e^{i\pi/4}}{\sqrt{8\pi\kappa}} u^{pr}(\mathbf{x}, \mathbf{d}) \quad \mathbf{x} \in D^c, \mathbf{d} \in \mathbb{S},$$

where $u^{pr} = -(\Delta u^{sc} - \kappa^2 u^{sc}) / (2\kappa^2)$.

Lemma 4.3. *The following relation holds*

$$|u^\infty(\hat{\mathbf{x}}, -\mathbf{d})| + |\partial_{\theta_{\hat{\mathbf{x}}}} u^\infty(\hat{\mathbf{x}}, -\mathbf{d})| \leq C \quad \hat{\mathbf{x}}, \mathbf{d} \in \mathbb{S},$$

where C is a constant which depends on the wave number κ and the domain D .

Proof. The proof can be easily derived by Lemma [2.1](#). □

The above lemmas shows that the asymptotic behaviors of the scattered field $u^{sc}(\mathbf{x}_r, \mathbf{x}_s)$ are very similar to the those of the acoustic scattered field with the same point sources as the incident field. Besides, the imaging function I_{11} is the same as that in the case of phaseless inverse acoustic scattering problem in the form. Thus we can use the same method in [8] to get the resolution analysis of the imaging function I_{11} . Here we omit the proof for brevity.

Theorem 4.4. *For any $\mathbf{z} \in \Omega$, it holds that*

$$I_{11}(\mathbf{z}) = I_1(\mathbf{z}) + w_{phaseless}(\mathbf{z}),$$

where $\|w_{phaseless}\|_{L^\infty(\Omega)} \leq CR_s^{-1/2}$.

We end this section by the following reconstruction algorithm:

Reconstruction algorithm for extended obstacles with phaseless data

- Choose a sampling domain Ω and generate sampling points.
- For each sampling point $\mathbf{z} \in \Omega$, calculate the imaging function $I_{11}(\mathbf{z})$.
- Plot the contours for the imaging function

$$\hat{I}_{11}(\mathbf{z}) = \frac{I_{11}(\mathbf{z})}{\max_{\mathbf{z} \in \Omega} I_{11}(\mathbf{z})}.$$

5 Numerical experiments

In this section, several numerical examples will be presented to show the feasibility of our algorithm. To get the synthetic data, we adopt the boundary integral equation method in [11]. For the noisy data, the following formula is used

$$u_\delta^{sc}(\mathbf{x}_r, \mathbf{x}_s) = u^{sc}(\mathbf{x}_r, \mathbf{x}_s) + \delta \frac{|u^{sc}(\mathbf{x}_r, \mathbf{x}_s)|}{|\xi_1 + i\xi_2|} (\xi_1 + i\xi_2),$$

where δ is the noise level, and ξ_1 and ξ_2 are random numbers subject to the standard normal distribution.

Example 1. We consider the case where the obstacle is a unit circle centered at the origin. The sampling domain Ω is $[-6, 6] \times [-6, 6]$ and the wave number is 2π . We use algorithm to reconstruct the obstacle; see figure [1](#). It can be seen from figure [1](#) that our algorithm based on these imaging functions can locate the obstacle effectively.

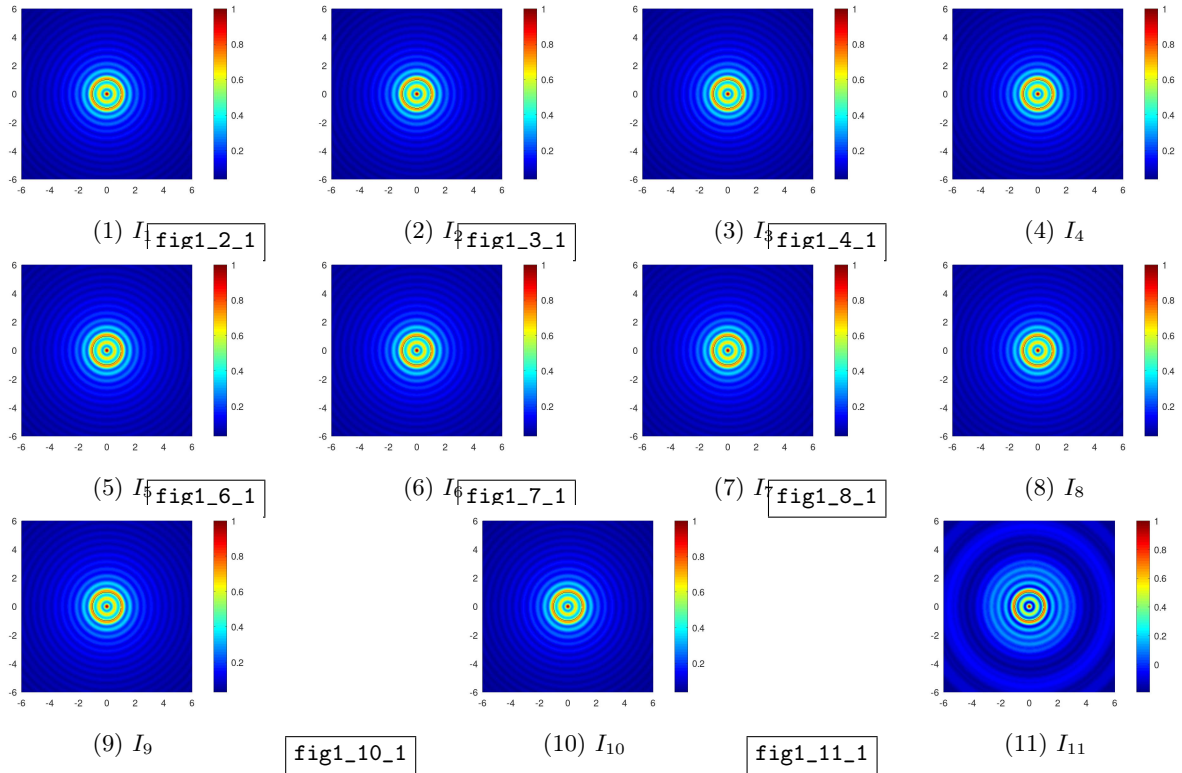
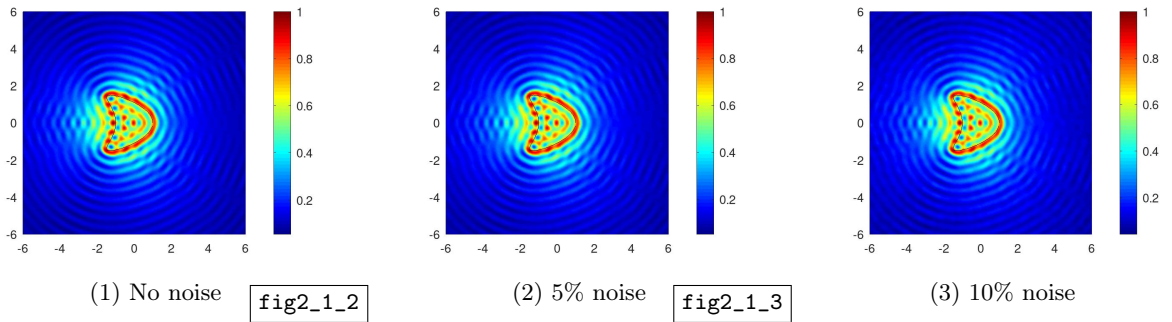


Figure 1: Example 1: The reconstruction results with no noisy data

Example 2. We consider the influence of noisy data. Assume that the obstacle D is a kite whose parameterized form is

$$(0.65 \cos(2t) + \cos t - 0.65, 1.5 \sin t) \quad t \in [0, 2\pi].$$

The sampling domain is $[-6, 6] \times [-6, 6]$ and the wave number κ is 2π . The results with noise level 0%, 5% and 10% are shown in figure 2, which demonstrate that our algorithm is robust to the noise.



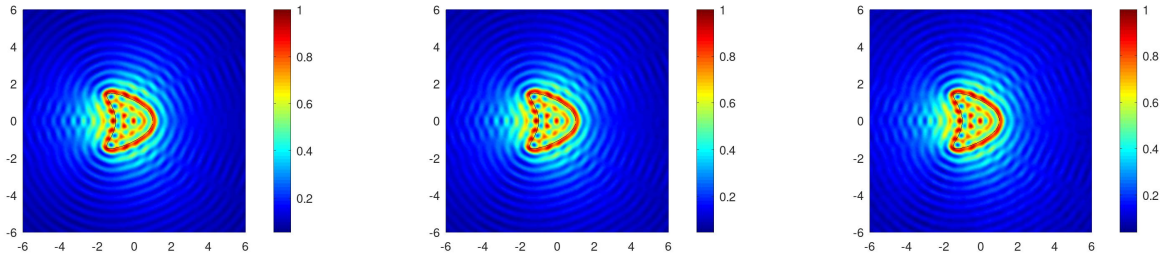
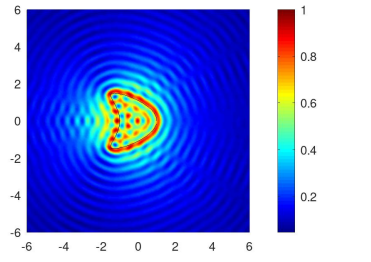


fig2_2_1

(4) No noise

fig2_2_2



(5) 5% noise

fig2_2_3

(6) 10% noise

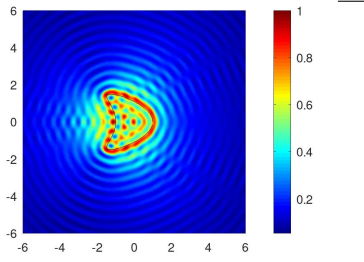
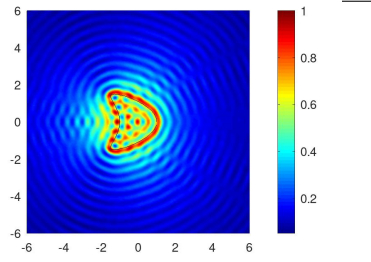


fig2_3_1

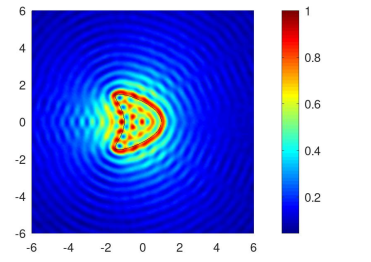
(7) No noise

fig2_3_2



(8) 5% noise

fig2_3_3



(9) 10% noise

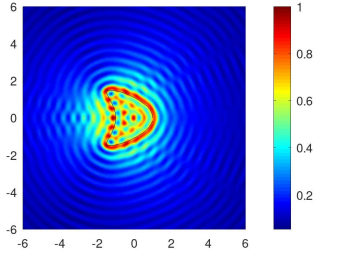
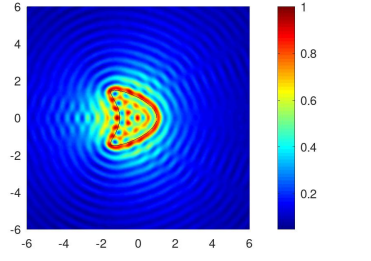


fig2_4_1

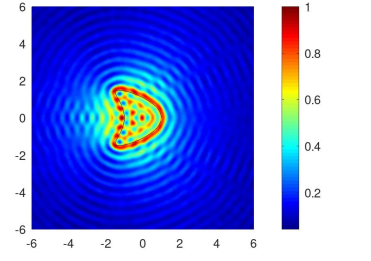
(10) No noise

fig2_4_2



(11) 5% noise

fig2_4_3



(12) 10% noise

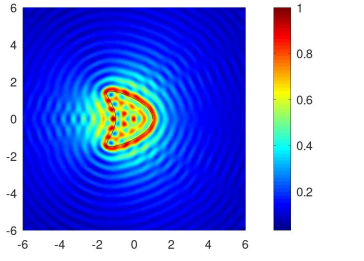
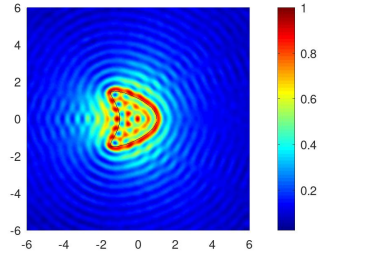


fig2_5_1

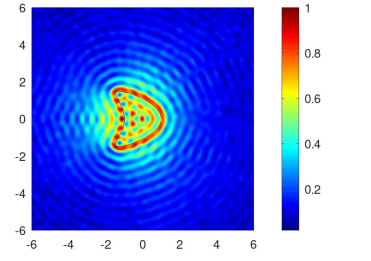
(13) No noise

fig2_5_2



(14) 5% noise

fig2_5_3



(15) 10% noise

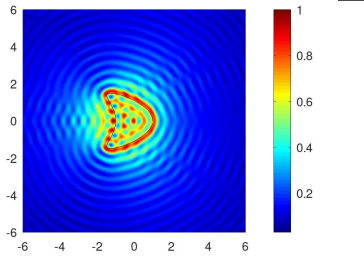
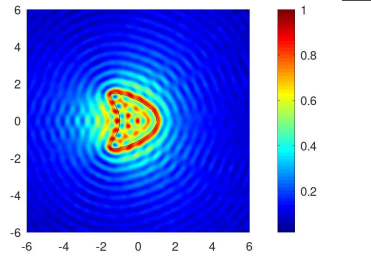


fig2_6_1

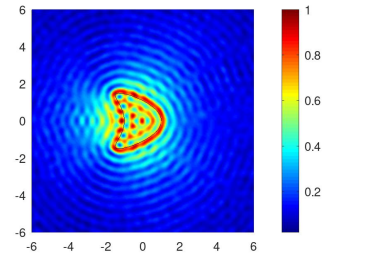
(16) No noise

fig2_6_2



(17) 5% noise

fig2_6_3



(18) 10% noise

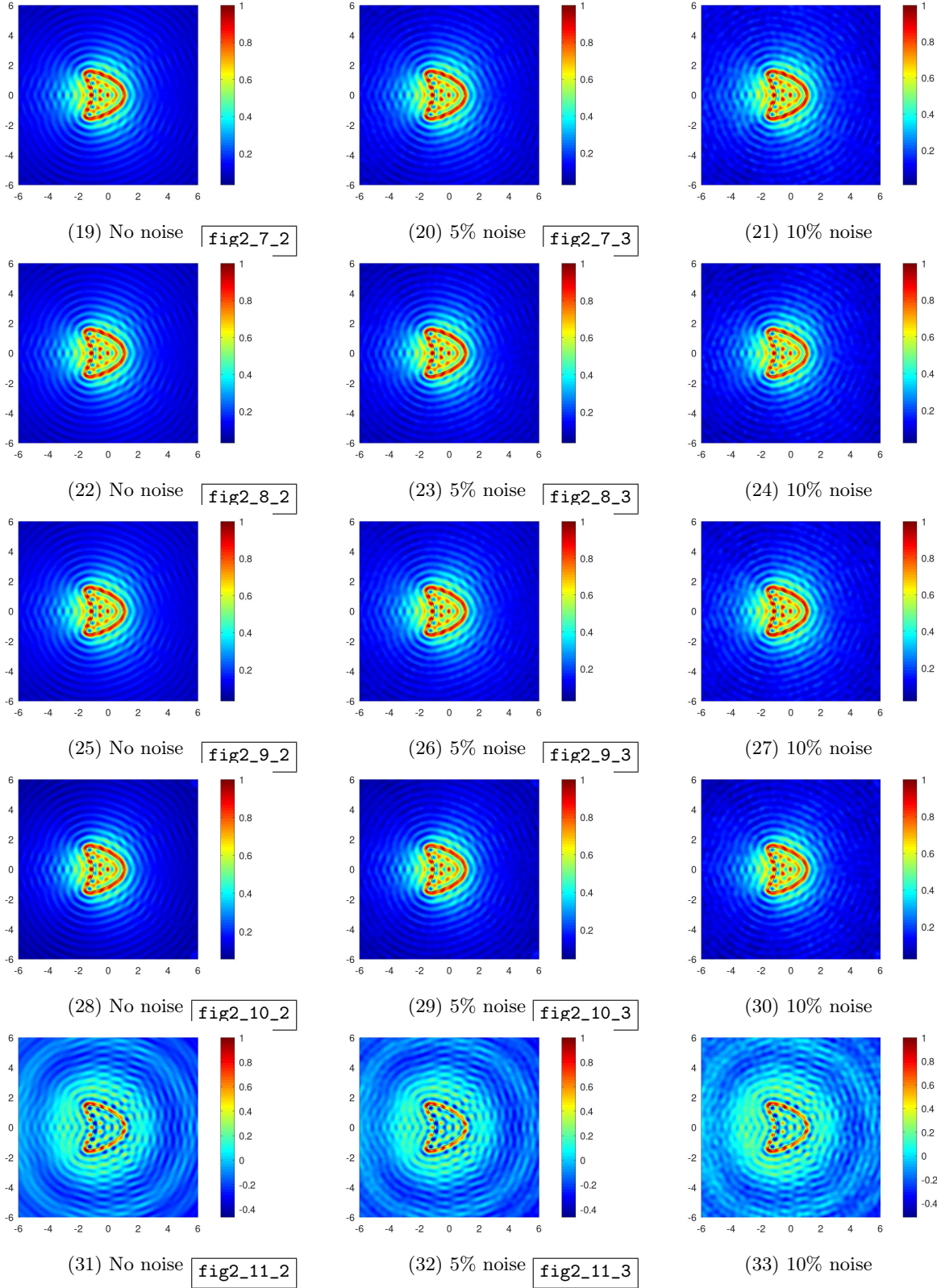
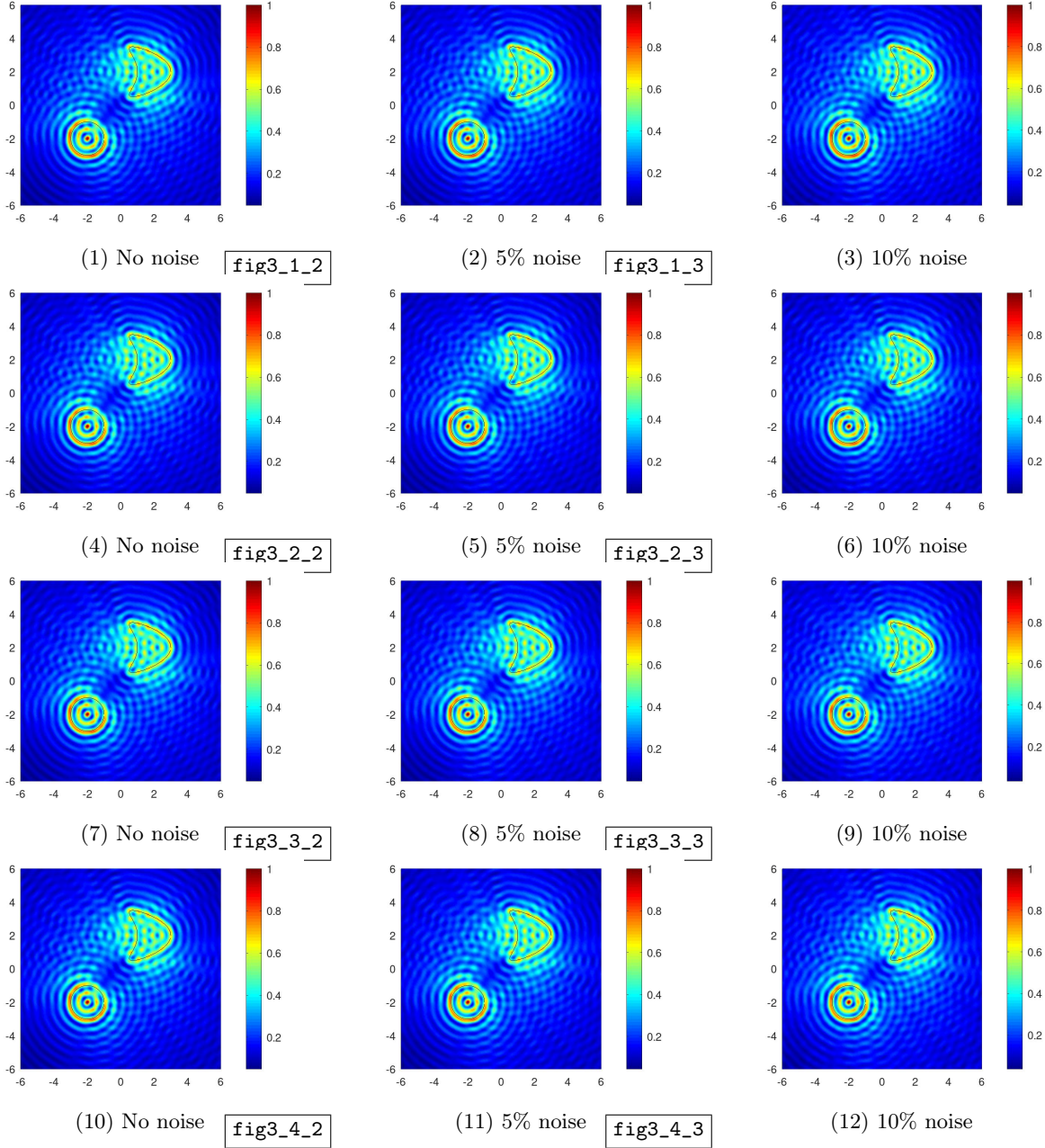


Figure 2: Example 2: The j -th row presents the reconstruction results of the indicator function I_j ($j = 1, \dots, 11$).

Example 3. We consider the case of two obstacles, i.e., a circle and a kite.

$$\begin{aligned} &(\cos t - 2, \sin t - 2) \quad t \in [0, 2\pi], \\ &(0.65 \cos(2t) + \cos t + 1.35, 1.5 \sin t + 2) \quad t \in [0, 2\pi]. \end{aligned}$$

The sampling domain is $[-6, 6] \times [-6, 6]$ and the wave number κ is 2π . The reconstruction results are presented in figure 3. Clearly, our algorithm also works well for multiple obstacles.



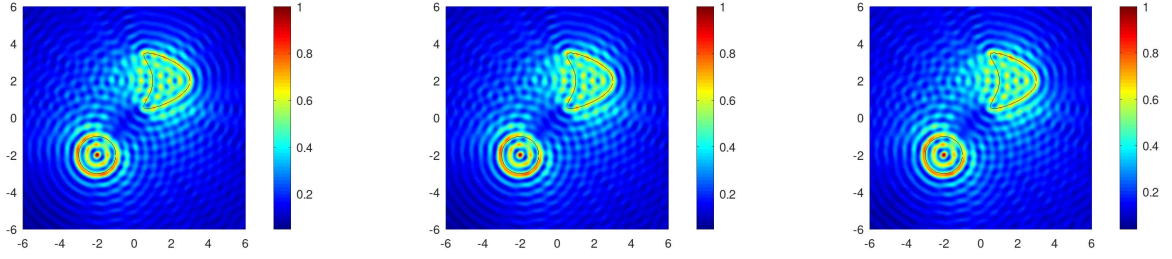


fig3_5_1

(13) No noise

fig3_5_2

(14) 5% noise

fig3_5_3

(15) 10% noise

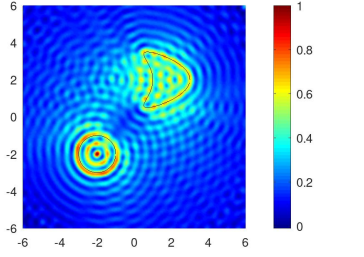


fig3_6_1

(16) No noise

fig3_6_2

(17) 5% noise

fig3_6_3

(18) 10% noise

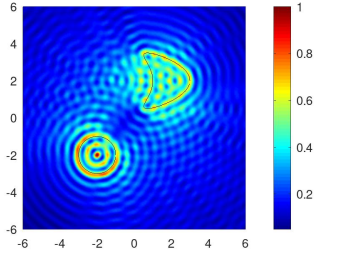


fig3_7_1

(19) No noise

fig3_7_2

(20) 5% noise

fig3_7_3

(21) 10% noise

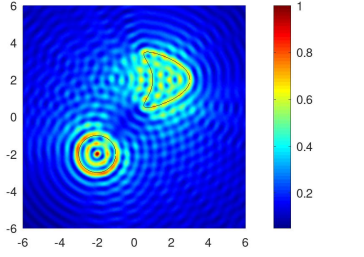


fig3_8_1

(22) No noise

fig3_8_2

(23) 5% noise

fig3_8_3

(24) 10% noise

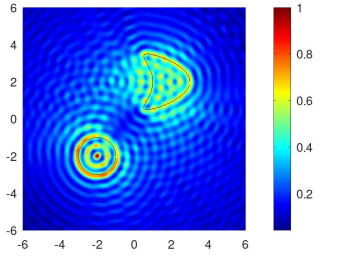


fig3_9_1

(25) No noise

fig3_9_2

(26) 5% noise

fig3_9_3

(27) 10% noise

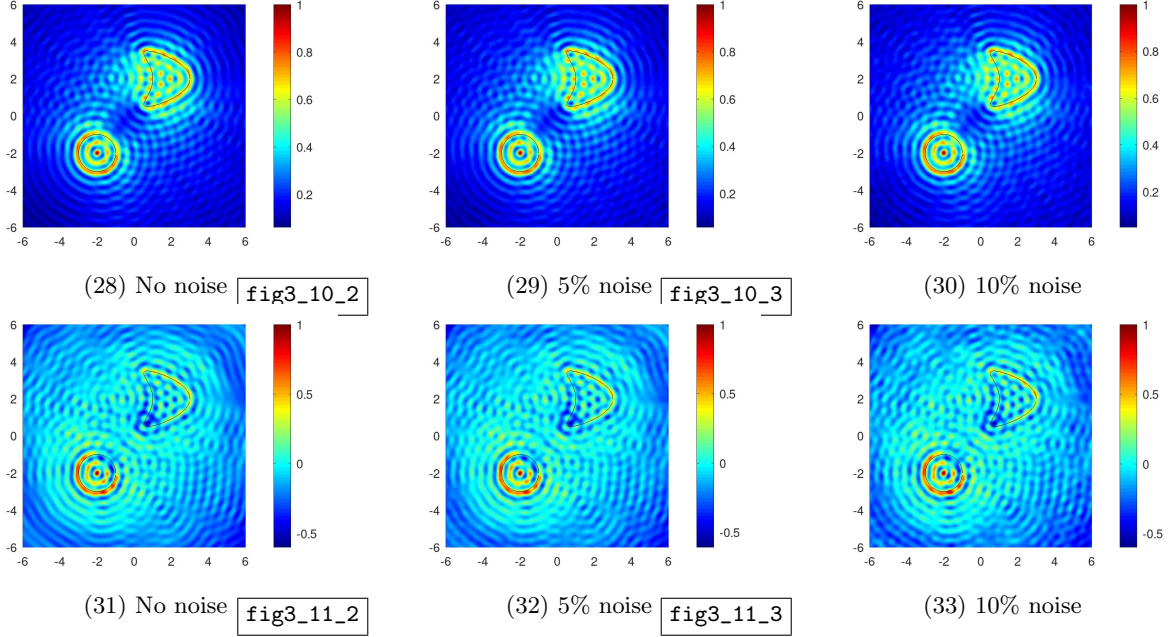


Figure 3: Example 3: The j -th row presents the reconstruction results of the indicator function I_j ($j = 1, \dots, 11$).

Acknowledgments

The research of TZ is supported by the Natural Science Foundation of Henan Province (No. 242300421677). The resaearch of ZG is supported by the National Natural Science Foundation of China (No. 12371393) and Natural Science Foundation of Henan Province (No. 242300421047).

References

- [1] Bourgeois L and Hazard C 2020 On well-posedness of scattering problems in a Kirchhoff-Love infinite plate *SIAM J. Appl. Math.* **80** 1546-66
- [2] Bourgeois L and Recoquilly A 2020 The linear sampling method for Kirchhoff-Love infinite plates *Inverse Probl. Imaging* **14** 363-84
- [3] Cakoni F, Colton D and Monk P 2011 *The Linear Sampling Method in Inverse Electromagnetic Scattering* (Society for Industrial and Applied Mathematics)
- [4] Chang Y and Guo Y 2023 An optimization method for the inverse scattering problem of the biharmonic wave *Commun. Anal. Comput.* **1** 168-82
- [5] Chen J, Chen Z and Huang G 2013 Reverse time migration for extended obstacles: Acoustic waves *Inverse Problems* **29** 085005
- [6] Chen J, Chen Z and Huang G 2013 Reverse time migration for extended obstacles: Electromagnetic waves *Inverse Problems* **29** 085006
- [7] Chen Z and Huang G 2015 Reverse time migration for extended obstacles: Elastic waves *Sci. Sin. Math.* **45** 1103-14

- aseless_2017 [8] Chen Z and Huang G 2017 Phaseless imaging by reverse time migration: Acoustic waves *Numer. Math. Theory Methods Appl.* **10** 1-21
- boundary_2010 [9] Chen G and Zhou J 2010 *Boundary Element Methods with Applications to Nonlinear Problems* (Atlantis Press; World Scientific)
- inverse_2019 [10] Colton D and Kress R 2019 *Inverse Acoustic and Electromagnetic Scattering Theory* 4th edn (Springer)
- g_novel_2024 [11] Dong H and Li P 2024 A novel boundary integral formulation for the biharmonic wave scattering problem *J. Sci. Comput.* **98** 42
- queness_2024 [12] Dong H and Li P 2024 Uniqueness of an inverse cavity scattering problem for the time-harmonic biharmonic wave equation *Inverse Problems* **40** 065011
- inverse_2023 [13] Gao Y, Liu H and Liu Y 2023 On an inverse problem for the plate equation with passive measurement *SIAM J. Appl. Math.* **83** 1196-214
- _direct_2025 [14] Guo J, Long Y, Wu Q and Li J 2024 On direct and inverse obstacle scattering problems for biharmonic waves *Inverse Problems* **40** 125032
- _direct_2025 [15] Harris I, Lee H and Li P 2025 Direct sampling for recovering a clamped cavity from the biharmonic far-field data *Inverse Problems* **41** 35013
- _direct_2022 [16] Harris I, Nguyen D-L and Nguyen T-P 2022 Direct sampling methods for isotropic and anisotropic scatterers with point source measurements *Inverse Probl. Imaging* **16** 1137-62
- _newton_1998 [17] Hohage T and Schormann C 1998 A Newton-type method for a transmission problem in inverse scattering *Inverse Problems* **14** 1207-27
- boundary_2021 [18] Hsiao G C and Wendland W L 2021 *Boundary Integral Equations* (Springer International Publishing)
- _direct_2012 [19] Ito K, Jin B and Zou J 2012 A direct sampling method to an inverse medium scattering problem *Inverse Problems* **28** 025003
- acoustic_2019 [20] Ji X, Liu X and Zhang B 2019 Inverse acoustic scattering with phaseless far field data: Uniqueness, phase retrieval, and direct sampling methods *SIAM J. Imag. Sci.* **12** 1163-89
- rization_2008 [21] Kirsch A and Grinberg N 2008 *The Factorization Method for Inverse Problems* (Oxford University Press)
- _Stable_2023 [22] Lan T H and Nguyen D-L 2023 Stable reconstruction of anisotropic objects from near-field electromagnetic data (arXiv:2309.12606)
- u_novel_2017 [23] Liu X 2017 A novel sampling method for multiple multiscale targets from scattering amplitudes at a fixed frequency *Inverse Problems* **33** 085011
- numerical_2023 [24] Nguyen D-L and Truong T 2023 On the numerical solution to an inverse medium scattering problem *Acta Math. Vietnam.* **48** 551-66
- mpyrotic_1974 [25] Olver F W J 1974 *Asymptotics and Special Functions* (Academic Press)
- obstacle_2024 [26] Wu C and Yang J 2024 The obstacle scattering for the biharmonic equation (arXiv:2406.06126)
- st_study_2010 [27] Potthast R 2010 A study on orthogonality sampling *Inverse Problems* **26** 074015
- bayesian_2020 [28] Yang Z, Gui X, Ming J and Hu G 2020 Bayesian approach to inverse time-harmonic acoustic scattering with phaseless far-field data *Inverse Problems* **36** 65012
- roximate_2020 [29] Zhang B and Zhang H 2020 An approximate factorization method for inverse acoustic scattering with phaseless total-field data *SIAM J. Appl. Math.* **80** 2271-98